Leishmania uses Mincle to target an inhibitory ITAM signaling pathway in dendritic cells that dampens adaptive immunity to infection

Salvador Iborra[1,2,9,*], María Martínez-López[1,9], Francisco J. Cueto[1,3], Ruth Conde-Garrosa[1], Carlos Del Fresno[1], Helena M. Izquierdo[1], Clare L. Abram[4], Daiki Mori[5], Yolanda Campos-Martín[6], Rosa María Reguera[7], Benjamin Kemp[8], Sho Yamasaki[5], Matthew J. Robinson[8], Manuel Soto[2], Clifford A. Lowell[4] and David Sancho[1, 10, *].

[1] Immunobiology laboratory. Fundación Centro Nacional de Investigaciones Cardiovasculares "Carlos III" (CNIC), Melchor Fernández Almagro 3, Madrid, 28029, Spain
[2] Departamento de Biología Molecular Centro de Biología Molecular Severo Ochoa (CSIC-UAM), Nicolás Cabrera 1, Universidad Autónoma de Madrid, Madrid, 28049, Spain
[3] Department of Biochemistry, Faculty of Medicine, Universidad Autónoma de Madrid, Calle Arzobispo Morcillo 4, Madrid, 28029, Spain
[4] Department of Laboratory Medicine, University of California, San Francisco, CA 94143, USA
[5] Division of Molecular Immunology, Medical Institute of Bioregulation, Kyushu University, Fukuoka 812-8582, Japan.
[6] Servicio Anatomía Patológica, Hospital Virgen de la Salud, Av. Barber, 30, Toledo, 45004, Spain
[7] Departamento de Ciencias Biomédicas, Universidad de León, Facultad de Veterinaria Campus de Vegazana s/n, León, 24071, Spain
[8] Medimmune, Granta Park, Cambridge. CB21 6GH, United Kingdom
[9] Co-first author
[10] Lead Contact

[*] Correspondence: siborra@cnic.es (S.I.), dsancho@cnic.es (D.S.)
Immunobiology Laboratory
Centro Nacional de Investigaciones Cardiovasculares Carlos III (CNIC)
Melchor Fernández Almagro, 3
E-28029, Madrid, Spain
Tel: (+ 34) 914531200 Ext 2010
Tel (direct line): (+ 34) 662 990 4777 2010
FAX: (+ 34) 914531245

Summary

C-type lectin receptors sense a diversity of endogenous and exogenous ligands that may trigger differential responses. Here, we have found that human and mouse Mincle bind to a ligand released by *Leishmania*, a eukaryote parasite that evades an effective immune response. Mincle-deficient mice had milder dermal pathology and a tenth of the parasite burden compared to wild-type mice after *Leishmania major* intradermal ear infection. Mincle deficiency enhanced adaptive immunity against the parasite, correlating with increased activation, migration and priming by Mincle-deficient dendritic cells (DCs). *Leishmania* triggered a Mincle-dependent inhibitory axis characterized by SHP1 coupling to the FcRγ chain. Selective loss of SHP1 in $CD11c^{+}$ cells phenocopies enhanced adaptive immunity to *Leishmania*. In conclusion, *Leishmania* shifts Mincle to an inhibitory ITAM (ITAMi) configuration that impairs DC activation. Thus, ITAMi can be exploited for immune evasion by a pathogen and may represent a paradigm for ITAM-coupled receptors sensing self and non-self.

Introduction

C-type lectin receptors (CLRs) are equipped with the C-type lectin domain, a versatile structure for binding diverse ligands that allows sensing of self and non-self (Dambuza and Brown, 2015; Sancho and Reis e Sousa, 2012). Eukaryote parasites, such as *Leishmania*, are detected by CLRs, Toll-like receptors, and opsonizing antibodies via Fc receptors, which trigger a combination of activating and inhibitory pathways (Lefèvre et al., 2013; Woelbing et al., 2006). Mice infected intradermally with *Leishmania major* develop lesions similar to those seen in patients with localized cutaneous leishmaniasis (Belkaid et al., 2000). *L. major* is a poor inducer of dendritic cell (DC) activation and inhibits migration of DCs to draining lymph nodes (dLNs) (Ng et al., 2008; Ribeiro-Gomes et al., 2012), although DCs do eventually migrate and promote T helper 1 (Th1) cell immunity and macrophage microbicidal activity (Leon et al., 2007). The mechanisms by which *Leishmania* initially blunts DC activation and T cell priming remain ill-defined. It has been argued that they may involve uptake of apoptotic infected neutrophils by DCs (Ribeiro-Gomes et al., 2012) or direct DC contact with parasite products (Srivastav et al., 2012). However, the receptor(s) mediating *L. major*-induced DC suppression have not been identified.

Mincle (macrophage-inducible C-type lectin, also known as Clec4e or Clecsf9) (Matsumoto et al., 1999) is weakly expressed in myeloid cells, including DCs, and is induced upon their activation in a macrophage C-type lectin (MCL, Clec4d, Clecsf8)-dependent fashion (Miyake et al., 2013; Yamasaki et al., 2008). Mincle was identified as an FcRγ chain-coupled CLR for endogenous SAP-130 exposed and released by dead cells (Yamasaki et al., 2008) but also recognizes glycolipids on the cell walls of bacteria and fungi, including trehalose-6, 6-dimycolate (TDM) and its synthetic analogue trehalose-6, 6-dibehenate (TDB) (Ishikawa et al., 2009; Ishikawa et al., 2013; Schoenen

et al., 2010; Wells et al., 2008; Yamasaki et al., 2009). Binding of these ligands to Mincle triggers phosphorylation of immunoreceptor tyrosine-based activation motif (ITAM) tyrosine residues in the FcRγ chain by Src-family kinases, followed by the recruitment and activation of the kinase Syk, which is facilitated by the phosphatase SHP2 as a scaffold (Deng et al., 2015). Subsequently, Syk generates an activating signal mediated by the protein CARD9 that boosts immunity to infections and inflammation in response to bacterial adjuvants (Ishikawa et al., 2009; Schoenen et al., 2010; Shenderov et al., 2013; Sousa et al., 2011; Yamasaki et al., 2009). Classically considered an activating CLR, Mincle has recently been associated with dampening of immunity (Seifert et al., 2016; Wevers et al., 2014; Wuthrich et al., 2015), acting by repressing IL12-p35 transcription through a Syk-Akt-PKB-dependent pathway in response to *Fonsecaea* (Wevers et al., 2014).

Here, we have found that loss of Mincle resulted in reduced parasitemia and enhanced immunity to *L. major*, correlating with stronger DC activation, priming and migration to dLN. *Leishmania* released a soluble proteinaceous Mincle ligand and induced a Mincle-dependent inhibitory axis. This inhibitory axis involved transient Syk activation that mediated coupling of SHP1 to FcRγ chain and dampened DC activation. Recruitment of SHP1 to the ITAM and mediating inhibitory signaling toward heterologous receptors (inhibitory ITAM, ITAMi) have been described for Fc receptors binding monomeric immunoglobulins (Aloulou et al., 2012; Ben Mkaddem et al., 2014; Hamerman et al., 2009; Pasquier et al., 2005), but not downstream of pattern recognition receptors. Our results reveal the relevance of the ITAMi pathway activated via Mincle after detection of a pathogen and as a mechanism of immune evasion by *L. major*. This ligand-dependent dual sensing and activation of the ITAM domain may be

a paradigm for other ITAM-coupled receptors that have to deal with diverse exogenous and endogenous ligands.

Results

Leishmania releases a soluble proteinaceous ligand for Mincle

While screening for pathogens expressing Mincle ligands by dot blot, we found that the human Mincle ectodomain-Fc chimera (Mincle-Fc) specifically bound soluble *Leishmania major* extracts from freeze-thawed promastigotes (Figure 1A, left). Mincle-Fc also bound to blotted supernatants from *L. major* promastigotes kept for 3h at 37ºC to favor secretion (Figure 1A, right) and detected plated soluble *Leishmania* antigen (SLA) or supernatants (SN) by ELISA (Figure 1B); in contrast, control-Fc or macrophage C-type lectin (MCL)-Fc did not bind to blotted or plated *Leishmania* extracts (Figure S1A). Loss of binding upon boiling of the parasite preparations indicated that the ligand is heat-sensitive (Figure 1A, B). Treatment of plated *Leishmania* extract with sodium periodate, which oxidizes glycans, did not affect binding of Mincle-Fc to the *Leishmania* extract, but did inhibit the trehalose-dependent binding to TDM (Figure S1B).

To determine whether the ligand bound cellular Mincle, B3Z NFAT reporter cells (Karttunen et al., 1992) were transduced with a chimera comprising the extracellular human Mincle and intracellular CD3ζ, or alternatively with the wild type (WT) mouse Mincle receptor co-transduced with the FcRγ chain and Syk. The CD3ζ chimera responds to any multimeric ligand, whereas WT Mincle requires the Syk kinase transduction pathway to activate an NFAT reporter (Sancho et al., 2009). Plated

Leishmania lysates triggered the Mincle-CD3ζ reporter, but not the WT Mincle-FcRγ-Syk or the parental cell line (Figure 1C). SLA did not trigger the Mincle-CD3ζ chimera or the WT Mincle (not shown), suggesting a low valency of the soluble ligand. In contrast, SLA blocked the triggering of WT Mincle or CD3ζ chimera by plated TDB in a dose-dependent and heat-sensitive manner (Figure 1D and not shown). SLA-mediated blockade did not affect the triggering of Mincle by plated 1B6 anti-Mincle antibody, indicating specificity for a TDB-Mincle binding site (Figure S1C). In addition, fluorochrome-labeled SLA bound to Mincle-expressing B3Z cells, but not to the parental cell line (Figure 1E and not shown).

Mincle-Fc also stained fixed and permeabilized *L. major* promastigotes, whereas Dectin-1-Fc did not (Figure 2A and S2A). Binding of Mincle-Fc to fixed and permeabilized *L. major* was specifically inhibited by preincubation of the ectodomain with 2F2 anti-Mincle or with soluble TDM (Figure 2B and S2B), but not with 1B6 anti-Mincle (not shown). Moreover, treatment of fixed and permeabilized *Leishmania* promastigotes with proteinase K, trypsin, heat, or low pH, but not DNaseI, inhibited labeling by Mincle-Fc chimera, suggesting a proteinaceous nature of the ligand (Figure 2C). Notably, other *Leishmania* species were also specifically stained by Mincle-Fc (Figure S2C).

Confocal analysis of Mincle-Fc staining in fixed and permeabilized *L. major* promastigotes revealed an intracellular granular pattern, including the flagellar pocket close to the kinetoplast, a unique site for exocytosis (Figure 2D). Mincle-Fc also stained the parasitophorous vacuole containing *L. major* amastigotes after uptake of the parasite by cultured macrophages (Figure 2E), alongside the staining of the endogenous nuclear ligand for Mincle (Yamasaki et al., 2008). Dectin-1 Fc did not stain fixed and

permeabilized promastigotes or amastigotes (Figure 2D and E) but did label endocytosed zymosan (Figure S2D). Thus, Leishmania produced a proteinaceous ligand(s) for Mincle that was detected in all tested *Leishmania* species and was present at both the promastigote and amastigote stages.

Mincle is expressed during *Leishmania* infection

The typical route of *Leishmania* infection is a skin bite by a parasite-inoculated sandfly. We therefore analyzed Mincle expression in dermal cell types of WT and Mincle-deficient (*Clec4e*$^{-/-}$) mice after *L. major* infection. The pinnae of both ears were inoculated by intradermal (i.d.) injection of 1000 *L. major* metacyclic promastigotes, and ear infiltrates were analyzed 24 hours later and compared with dermis taken from the ears of uninfected mice. Mincle expression by myeloid cells was modest in unchallenged dermis (Figure 3A and S3A) but was upregulated upon *L. major* infection in tissue macrophages, neutrophils, and monocyte-derived DCs (MoDCs) infiltrating the infection site (Figure 3A and B) and was maintained throughout the course of infection (Figure 3B). Mincle staining of myeloid cells was also observed in human skin samples and serial spleen sections from patients infected with *Leishmania infantum* (Figure S3B and C).

Mincle deficiency increases resistance to cutaneous leishmaniasis

To determine the contribution of Mincle to the immune response against *L. major*, we monitored cutaneous disease during an 11-week period after ear inoculation with 1000 *L. major* metacyclic promastigotes in WT or *Clec4e*$^{-/-}$ mice. In the first 2 weeks after infection, the inflammatory pathology in *Clec4e*$^{-/-}$ mice was similar to or greater than that in WT mice, but the response subsequently plateaued and there was no

development of dermal lesions (Figure 3C). A similar pathology was provoked with inoculation of 5 x 10^4 parasites (Figure S3D and E), the dose subsequently used to induce a robust adaptive response in the challenge region. Since the third week of infection, parasite loads in the ears and dLNs of *Clec4e*$^{-/-}$ mice were 90% lower than those of their WT counterparts (Figure 3D and E). Real-time tracking of i.d. ear infection with *L. major* mCherry confirmed better control of infection was in *Clec4e*$^{-/-}$ mice, with significantly lower parasite load at all times analyzed (Figure 3F). Mincle-deficient mice thus controlled the infection earlier and more effectively than WT mice, leading to reduced pathology.

Mincle deficiency strengthens the adaptive response to *L. major*

Polyclonal effector CD4$^+$ T cells producing IFN-γ (but not CD8$^+$ T cells) were significantly more abundant in the ears of infected *Clec4e*$^{-/-}$ mice at 3, 6 and 10 weeks p.i. (Figure 4A and Figure S4A). CD4$^+$ T cells present in dLNs from infected *Clec4e*$^{-/-}$ mice showed augmented production of IFN-γ, but not IL-10, in response to SLA (Figure 4B and Figure S4B). The strong Th1 effector CD4$^+$ T cell response also correlated with higher anti-*Leishmania* IgG2a but not IgG1 antibodies in *Clec4e*$^{-/-}$ mice (Figure S4C).

To investigate the mechanism of the enhanced adaptive response to *L. major* in the absence of Mincle, we analyzed early CD4$^+$ T cell priming. As described (Pagán et al., 2013; Ribeiro-Gomes et al., 2012), infection with *L. major* expressing the model antigen ovalbumin (OVA) induced poor priming of OVA-specific CD4$^+$ T cells (Figure 4C). Priming was boosted in *Clec4e*$^{-/-}$ mice, with enhanced CD4$^+$ T cell proliferation *in vivo* and IFN-γ production upon OVA restimulation *ex vivo* (Figure 4C, D, and Figure S4D). The specificity of the Mincle-dependent decrease in CD4$^+$ T cell priming for *L. major* was confirmed by identical effector responses in WT and *Clec4e*$^{-/-}$ mice upon

infection with OVA-expressing vaccinia virus (Figure 4C, D, and Figure S4D). These data show that *Leishmania* targets Mincle to decrease priming of a $CD4^+$ Th1 cell-type response against the parasite.

To determine the relevance of enhanced priming in a context of vaccination, we transferred OVA-specific $CD4^+$ T cells i.v. and subsequently injected 1 x 10^5 freeze-thawed *L. major*-OVA i.d. into the ear. Injection of dead parasites into *Clec4e*$^{-/-}$ mice resulted in increased numbers of OVA-specific $CD4^+$ T cells producing IFN-γ upon restimulation *ex vivo* (Figure 4E and Figure S4E). We next analyzed whether Mincle deficiency also strengthens the function of the memory $CD4^+$ T cell compartment. Vaccination with freeze-thawed *Leishmania* followed by *L. major* rechallenge 4 weeks later induced IFN-γ^+ $CD4^+$ effector T cells in the ear of *Clec4e*$^{-/-}$ but not WT mice (Figure 4F), thus generating a protective response with reduced parasitemia (Figure 4G). This Mincle-dependent vaccination deficiency using freeze-thawed *Leishmania* extracts in WT mice could be reverted by the use of CpG as adjuvant (Figure 4F and G), consistent with published findings (Walker et al., 1999). These results indicated that upon sensing *Leishmania*, Mincle inhibited the generation of effector and memory $CD4^+$ T cells and impaired the adaptive response to *L. major*.

Mincle absence increases DC activation and migration to dLNs after *L. major* infection

Given the increased adaptive response, we next investigated whether Mincle-deficient DCs had an enhanced ability to prime anti-*L. major* responses. DCs extracted from dLNs of *Clec4e*$^{-/-}$ mice were better than WT at restimulating *L. major*-specific $CD4^+$ T cells obtained from healed WT mice (Figure 5A). Early after *L. major* infection, CD40 expression on DCs in the ear was significantly upregulated in *Clec4e*$^{-/-}$ mice compared

with WT mice (Figure S5A). Moreover, MoDCs infiltrating the dermis of Mincle-deficient mice also showed upregulation of the activation markers CD40 and CD86 and the chemokine receptor CCR7 at 20h and 14d after infection (Figure 5B).

In addition, *L. major* infection decreased the numbers of migratory DCs in a Mincle-dependent manner (Figure 5C). The effect of Mincle on the capacity of dermal DCs to migrate to the dLNs was further investigated in FITC skin sensitization assays. *L. major* infection inhibited migration of $FITC^+$ $CD11c^+$ DCs to dLNs in WT mice but not in *Clec4e*$^{-/-}$ mice (Figure 5D). Mincle-dependent inhibition of DC migration was maintained two weeks after infection (Figure S5B). These results suggest that *Leishmania* sensing by Mincle impaired DC activation in the infection site and subsequently limited their capacity to migrate to dLNs, contributing to the reduced priming to *L. major* in the presence of Mincle.

L. major promotes a Mincle- and SHP1-dependent inhibitory axis in DCs

To test whether increased DC activation in the absence of Mincle was intrinsic, we generated GMCSF bone-marrow-derived cells akin to DCs (GM-DCs) from WT and *Clec4e*$^{-/-}$ mice (Figure S6A). Stimulation with freeze-thawed *L. major* induced increased expression of CD40, CD86 and CCR7 in Mincle-deficient $CD11c^+$ GM-DCs (Figure 6A and 6B, and S6B and S6C), suggesting an intrinsic effect. As Syk is downstream Mincle (Yamasaki et al., 2008), we tested the absence of Syk in the CD11c compartment (CD11cΔ*Syk*) (Iborra et al., 2012). GM-DCs from CD11cΔ*Syk* mice showed impaired activation by freeze-thawed *L. major* (Figure 6B and S6C), suggesting the possible existence of an unidentified activating Syk-coupled DC receptor for *L. major* (Lefèvre et al., 2013).

MCL and Mincle are mutually regulated and act as heterodimers for binding to TDM (Kerscher et al., 2016; Lobato-Pascual et al., 2013; Miyake et al., 2015; Miyake et al., 2013). Consistent with these reports, GM-DCs derived from *Clec4d*$^{-/-}$ mice lacked expression of not only MCL but also Mincle (Figure S6D). Mincle expression was rescued by transduction with WT MCL or MCL^{WAA} (Figure S6D), which contains a mutation in calcium-binding motif of the C-type lectin domain (Miyake et al., 2015). The impaired expression of Mincle and MCL in *Clec4d*$^{-/-}$ mice resulted in increased activation of DCs exposed to freeze-thawed *L. major* (Figure 6C). Reexpression of Mincle mediated by transduction of both MCL or MCL^{WAA} correlated with impaired DC activation by *L. major* (Figure 6C), suggesting that regulation of Mincle expression by MCL contributes to responses to *L. major*.

Infection with *Fonsecaea* triggers Akt-dependent repression of IL12p35 transcription (Wevers et al., 2014). In contrast, freeze-thawed *L. major* did not induce Akt activation in WT mice (Figure S6E). We hypothesized that DC activation by *L. major* might be antagonized by Mincle through the recruitment of SHP1 in an inhibitory ITAM (ITAMi) configuration (Aloulou et al., 2012; Ben Mkaddem et al., 2014; Hamerman et al., 2009; Pasquier et al., 2005). Consistent with this notion, treatment with the SHP1/2 phosphatase inhibitor NSC-87877 increased DC activation by *L. major* (Figure S6F), contrasting with the absence of an effect with the Akt inhibitor VIII. Notably, NSC-87877 did not further activate Mincle-deficient DCs in response to the parasite (Figure S6G), suggesting that Mincle and phosphatase activity act in the same pathway. Supporting this conclusion, the enhanced freeze-thawed *L. major*-mediated activation seen in Mincle-deficient mice was phenocopied in GM-DCs from mice lacking SHP1 in the CD11c compartment (CD11cΔ*SHP1*) (Abram et al., 2013) (Figure 6D and S6H). freeze-thawed *L. major*-induced cytokine production was also higher in

GM-DCs lacking Mincle or SHP1 (Figure 6E). Moreover, like *Clec4e*$^{-/-}$ mice tested in parallel, CD11cΔ*SHP1* mice displayed lower ear and LN parasitemia in response to *L. major* infection (Figure 6F) and showed increased adaptive immunity (Figure 6G). Thus, our results suggested that Mincle inhibited DC activation through SHP1.

L. major shifts Mincle to an inhibitory ITAM configuration that suppresses heterologous receptors

Participation of Mincle and SHP1 in the same axis was further supported by Mincle-dependent phosphorylation of SHP1 (but not SHP2) in freeze-thawed *L. major*-stimulated GM-DCs (Figure 7A and Figure S7A and B). Pull-down of SHP1 in WT or FcRγ-chain-deficient GM-DCs revealed specific FcRγ-dependent association of SHP1 with Mincle (Figure 7B). Notably, treatment of GM-DCs with plated TDB induced FcRγ-dependent association of Mincle with Syk, but not with SHP1 (Figure S7C). Moreover, pull-down of Mincle from B3Z transfectants expressing tyrosine mutants in the FcRγ ITAM domain demonstrated that the membrane-distal tyrosine 76 was crucial for association of Mincle-FcRγ with SHP1, whereas tyrosine 65 was at least partially dispensable (Figure 7C), consistent with the ITAMi configuration (Ben Mkaddem et al., 2014).

We next tested the effect of the *L. major*-induced Mincle-dependent inhibitory axis on GM-DC activation promoted by LPS. freeze-thawed *L. major* dampened LPS-induced activation in GM-DCs and this inhibition was dependent on Mincle and Syk (Figure 7D). The ITAMi configuration is dependent on transient activation of Syk (Ben Mkaddem et al., 2014). We found that Syk transiently associated with Mincle in GM-DCs stimulated with freeze-thawed *L. major* in a manner dependent on the FcRγ chain (Figure 7E). Notably, CD11cΔ*Syk* DCs showed impaired SHP1 recruitment to Mincle

(Figure 7F). These results suggest that *L. major* shifts Mincle to an ITAMi configuration that suppresses heterologous activating receptors, dampening DC activation and thus impairing the induction of adaptive immune responses.

Discussion

Parasites that depend on an invertebrate vector for cyclical transmission have evolved mechanisms to delay or prevent sterilizing immunity in vertebrate hosts, thereby prolonging parasite availability to the vector (Yazdanbakhsh and Sacks, 2010). *Leishmania* parasites replicate silently in the skin for several weeks after inoculation (Belkaid et al., 2000), suggesting that they might actively dampen DC recognition or activation (Srivastav et al., 2012) and establish a functional immune privilege in the skin (Peters and Sacks, 2006). In this study, we have found that *L. major* parasites release a soluble ligand that binds Mincle, triggering an ITAMi signaling pathway that suppresses DC activation by heterologous activating receptors concomitantly sensing *L. major*. Mincle deficiency thus favored stronger DC activation in response to *L. major* infection, manifested in higher expression of costimulatory molecules, migration to dLNs, and priming of a Th1 cell response to parasite antigens. Increased Th1 cell-type immunity correlated with reduced parasite load and pathology in Mincle-deficient mice. These results reveal how the ITAMi pathway can be targeted by a pathogen as a mechanism to evade immune surveillance, and illustrate a SHP1-based inhibitory pathway in an ITAM-coupled CLR.

Mincle is a FcRγ-Syk-coupled CLR (Kerscher et al., 2013; Sancho and Reis e Sousa, 2012, 2013) with a well-established role in inducing inflammation and host immunity in response to glycolipid ligands in the cell wall of bacteria and fungi

(Ishikawa et al., 2009; Ishikawa et al., 2013; Schoenen et al., 2010; Shenderov et al., 2013; Sousa et al., 2011; Wells et al., 2008; Yamasaki et al., 2009). However, recent reports point to an additional, negative role for Mincle in the control of immunity (Seifert et al., 2016; Wevers et al., 2014; Wuthrich et al., 2015). Mincle detection of *Fonsecaea* involves an Akt-dependent pathway that selectively impairs IL12p35 transcription (Wevers et al., 2014). Therefore, the finding that Mincle sensing of *Leishmania* induces global DC inhibition through a SHP1-dependent and Akt-independent pathway was highly unexpected.

Engagement of FcRγ chain-coupled receptors by low-affinity or avidity ligands may cause hypophosphorylation of ITAM domains and result in recruitment of SHP1, a configuration termed inhibitory ITAM (ITAMi) (Aloulou et al., 2012; Ben Mkaddem et al., 2014; Hamerman et al., 2009; Pasquier et al., 2005). Our results provide an example of a functional ITAMi coupled to a pattern recognition receptor and support the potential physiological relevance of this signaling module (Aloulou et al., 2012; Blank et al., 2009; Pasquier et al., 2005). Transient Syk activation is required for the ITAMi configuration (Ben Mkaddem et al., 2014). We found transient Syk association with Mincle following freeze-thawed *L. major* stimulation and we showed that Syk is indeed required for SHP1 recruitment to Mincle. However, we found that the overall response of CD11cΔ*Syk* DCs to freeze-thawed *L. major* was impaired, likely because Syk was required for intracellular signaling pathways by other pattern recognition receptors that mediate activating signals to the parasite. Consistent with the ITAMi configuration, SHP1 associated through the membrane distal tyrosine 76 (Ben Mkaddem et al., 2014), which was crucial for association of Mincle-FcRγ to SHP1. Notably, soluble *Leishmania* extract inhibited DC activation upon LPS challenge in a Mincle-dependent manner, showing the potential of this FcRγ/SHP1 axis to interfere with diverse

activating pathways through heterologous receptors, all these features defining the ITAMi pathway.

Given that the *Leishmania* ligand was soluble, avidity for Mincle could be reduced (Iborra and Sancho, 2015). In contrast to Leishmania ligand, we did not find SHP1 associated with Mincle when GM-DCs were treated with plated TDB. Together with Mincle, the CLR MCL binds to and is essential for TDM adjuvant potential (Furukawa et al., 2013; Miyake et al., 2013). Mincle, MCL and FcRγ form a heteromeric complex that facilitates signaling (Lobato-Pascual et al., 2013). In addition, MCL and Mincle mutually regulate their expression (Kerscher et al., 2016; Miyake et al., 2015; Miyake et al., 2013). Here, we have found that control of Mincle expression by MCL is required for dampening DC activation in response to *L. major*. Our results do not support a direct role for MCL in the recognition of *L. major* by Mincle, since MCL-Fc did not bind to *Leishmania* extract and its inhibitory effect on DCs was maintained with a MCL^{WAA} mutant in the lectin domain that allows Mincle expression (Miyake et al., 2015), although the possibility that MCL could contribute directly cannot be completely ruled out. Our data show that the *L. major* ligand triggers SHP-1 phosphorylation via Mincle in B3Z cells in the absence of MCL. It is therefore feasible that the signal triggered by binding of *L. major* ligand to Mincle (in homo or heteromeric configuration) could be weaker than that triggered by the binding of TDM-coated structures to the Mincle-MCL heteromer, and this weaker signaling may favor the ITAMi configuration.

The presence of a ligand for Mincle may contribute to the low effectiveness of candidate vaccines based on whole killed *Leishmania* or attenuated parasites (Duthie et al., 2012). Our results indicate that blocking Mincle or SHP1 during a vaccination setting may improve vaccine efficiency by allowing Th1 responses to be induced.

Moreover, our findings suggest that Mincle can couple to an activating ITAM or to an ITAMi configuration depending on the nature of the ligand, an idea that could apply to other ITAM-coupled CLRs with a diverse ligand range or that can heterodimerize with multiple receptors (Iborra and Sancho, 2015).

Experimental Procedures

Mice

Mouse colonies were bred at the CNIC under specific pathogen-free conditions. Colonies included C57BL/6, *Clec4e*$^{-/-}$ (B6.Cg-Clec4e$^{tm1.1Cfg}$) backcrossed more than 10 times to C57BL/6J-Crl (kindly provided by Scripps Research Institute, through R. Ashman and C. Wells, Griffiths University, Australia) (Wells et al., 2008), CD11cΔ*Syk* (Iborra et al., 2012), *Fcer1g*$^{-/-}$ (B6;129P2-*Fcer1g*^{tm1Rav}/J) from The Jackson Laboratory (Takai et al., 1994), CD11cΔ*SHP1* (Abram et al., 2013), and OT-II CD4^{+} TCR transgenic mice in C57BL/6 background (B6.Cg-Tg(TcraTcrb)425Cbn/J) and mated with B6/SJL expressing CD45.1 isoform to facilitate cell tracking. Animal studies were approved by the local ethics committee. All animal procedures conformed to EU Directive 2010/63EU and Recommendation 2007/526/EC regarding the protection of animals used for experimental and other scientific purposes, enforced in Spanish law under Real Decreto 1201/2005.

Leishmania parasite preparation, inoculation, and quantitation

For *Leishmania* challenge, parasites of different lines were cultured and kept in a virulent state as described (Martinez-Lopez et al., 2015). Mice were infected by i.d. inoculation of 1000 or 5×10^4 metacyclic *L. major* promastigotes into the dermis of both

ears (Martinez-Lopez et al., 2015). Lesion size in the ear and number of viable parasites was determined as described (Martinez-Lopez et al., 2015). The parasite load is expressed as the number of parasites in the whole organ.

Parasite preparation of protein extracts and binding to Mincle-Fc chimera

For preparation of soluble *Leishmania* extract, also known as soluble *Leishmania* antigen (SLA), approximately 10^9 promastigotes were harvested and washed twice in PBS. After 3 cycles of freezing and thawing, the suspension was centrifuged at 13,000 × g for 20 min at 4°C, and supernatant containing SLA was collected and stored at −80°C. Protein concentration was estimated by the Bradford method.

Freeze-thawed *L. major* parasites were prepared by 3 cycles of freezing and thawing of 10^8 stationary parasites in complete RPMI medium or PBS. Fixed and permeabilized *Leishmania* parasites were prepared by fixing 10^8 parasites with 0.5 ml of 4% paraformaldehyde and immediate addition of 0.5 ml 1% NP-40. After incubation for 10 min at room temperature, parasites were extensively washed with PBS. To obtain culture supernatants, stationary promastigotes were washed 3 times in phosphate buffer saline (PBS), resuspended at $5x10^8$ parasites/ ml in serum free DMEM, and incubated for 3 h at 37º C. Culture supernatants were collected by two steps of centrifugation, first at 1,500 ×g for 5 min at 4 °C, followed by a second step at 2,500 ×g for 10 min at 4 °C. Protein concentration was estimated by the Bradford method. For dot-blot determination of Mincle ligands in *Leishmania* extracts, protein samples were applied to 0.2 μm membranes (BioRad) using a vacuum dot blot apparatus (BioRad). To load different protein amounts in each dot, protein samples were serially diluted in PBS (1:3). Similarly, for ELISA, high-binding plates were loaded with protein samples serially diluted in PBS (1:3). Plates were incubated for 24 hours at 4ºC. Later, membranes and

plates were washed with PBS and incubated with blocking solution (2% defatted milk in PBS) for 120 minutes at room temperature, followed by incubation with Mincle-Fc chimera or control Fc (2μg/ml) for 2 hours. Membranes and plates were then incubated with anti-human IgG (Fc gamma-specific) conjugated to biotin. Membranes were imaged with the *LI-COR* Odyssey Infrared Imaging System.

Generation and assay of B3Z cell lines expressing Mincle and FcRγ chain mutants

B3Z cells (kindly provided by N. Shastri, University of California) express a β-gal reporter for nuclear factor of activated T cells (NFAT) (Karttunen et al., 1992). B3Z cells were transduced with retroviruses expressing FcRγ chain, Syk and mouse Mincle. FcRγ chain ITAM tyrosine 65 and 76 phenylalanine mutants were generated using the QuickChange lightning site-directed mutagenesis kit (Agilent). Binding of ligands can be detected by NFAT reporter activation and induction of β-gal activity. B3Z cells were plated in 96 well plates and incubated with plated TDB or anti-Mincle (1B6) in the presence or absence of *Leishmania* extract. Lysed parasites used in B3Z assays were opsonized with fresh serum from infected Balb/c mice for 2 hours at RT and washed twice with cold PBS. Before B3Z cell plating, promastigotes were seeded on plates coated with 50 μg/ml poly-L-Lysine (Sigma), for 30 minutes at 37 ºC.

After overnight culture, cells were washed in PBS, and LacZ activity was measured by lysis in CPRG (Roche)-containing buffer. Four hours later O.D. 595 nm was measured relative to O.D. 655 nm used as a reference.

Adoptive transfer and antigen presentation studies *in vitro*

For adoptive transfer experiments, $CD4^+$ T cells were purified from pooled spleens and lymph nodes of OT-II $CD4^+$ TCR transgenic mice by negative selection (Miltenyi

Biotec). Purified $CD4^+$ T cells were incubated at 5×10^6 cells/ml in PBS with 0.5 μM CellTrace™ *Violet* (Invitrogen) for 10 min at 37Cº. The reaction was stopped with 5% FCS PBS. CellTrace™ *Violet* -labeled purified $CD4^+$ OT-II T cells ($2–5\times10^5$) were transferred just after challenge in the ear dermis either with $5x10^4$ metacyclic promastigotes of *Leishmania*-OVA, rVACV-OVA (kindly provided by J. Yewdell, NIAID, Bethesda) or dead *Leishmania* OVA ($1x10^5$). Four days after adoptive transfer, the dLNs were removed, LN cell suspensions were prepared and seeded in the presence of 10 μm $I\text{-}A^b$-restricted OVA peptide (323-339) and brefeldin A. LN cells were stained and analyzed by intracellular flow cytometry. In some experiments, T cells were purified from retromaxillary LNs of infected and healed mice and co-cultured with DCs enriched form dLNs of mice infected 48h before. IFN-γ release was determined in culture supernatants 72h later.

Statistical analysis

The statistical analysis was performed using Prism software (GraphPad Software, Inc). Statistical significance for comparison between two sample groups with a normal distribution (Shapiro-Wilk test for normality) was determined by unpaired two-tailed Student's *t* test. Comparisons of more than two groups were made by one way ANOVA and Bonferroni post-Hoc test. Differences were considered significant at $p < 0.05$ was considered significant (* $p < 0.05$; ** $p < 0.01$; *** $p < 0.001$).

Author contributions

S.I., M.M-L, F.J.C., C.d.F, H.M.I, R.C., Y.C., and D.S. did the experiments; C.L.A., C.A.L., D.M., B.K., S.Y., M.J.R., R.R., and M.S. provided essential reagents. S.I. and D.S. conceived and designed experiments, analyzed data and wrote the manuscript. All the authors discussed the results and the manuscript.

Acknowledgements

We are grateful to C. Reis e Sousa, C. Ardavín, A. Corbí, A. Hidalgo, and members of the D.S. laboratory for discussions and critical reading of the manuscript. We thank the CNIC facilities, personnel and to S. Bartlett for editorial assistance. We are indebted to G. Brown, J. Willment, A. Corbí, J.Yewdell, N. Shastri, C. Wells, R. Ashman, H. Miyoshi, RIKEN BRC and the Scripps Research Institute for providing reagents. SI is funded by grant SAF2015-74561-JIN. Work in the D.S. laboratory is funded by the CNIC and grants from the Spanish Ministry of Economy and Competitiveness (MINECO, SAF-2013-42920R), the European Commission (635122-PROCROP H2020) and the European Research Council (ERC-2010-StG 260414). The CNIC is supported by the MINECO and the Pro-CNIC Foundation, and is a Severo Ochoa Center of Excellence (MINECO award SEV-2015-0505). Conflict of interest: M.J.R. and B.K. are employees of MedImmune and shareholders in the parent company Astrazeneca. The other authors declare no competing financial interests.

References

Abram, C.L., Roberge, G.L., Pao, L.I., Neel, B.G., and Lowell, C.A. (2013). Distinct Roles for Neutrophils and Dendritic Cells in Inflammation and Autoimmunity in motheaten Mice. Immunity *38*, 489-501.

Aloulou, M., Ben Mkaddem, S., Biarnes-Pelicot, M., Boussetta, T., Souchet, H., Rossato, E., Benhamou, M., Crestani, B., Zhu, Z., Blank, U.*, et al.* (2012). IgG1 and IVIg induce inhibitory ITAM signaling through FcγRIII controlling inflammatory responses. Blood *119*, 3084-3096.

Belkaid, Y., Mendez, S., Lira, R., Kadambi, N., Milon, G., and Sacks, D. (2000). A natural model of Leishmania major infection reveals a prolonged "silent" phase of parasite amplification in the skin before the onset of lesion formation and immunity. J. Immunol. *165*, 969-977.

Ben Mkaddem, S., Hayem, G., Jonsson, F., Rossato, E., Boedec, E., Boussetta, T., El Benna, J., Launay, P., Goujon, J.M., Benhamou, M.*, et al.* (2014). Shifting FcgammaRIIA-ITAM from activation to inhibitory configuration ameliorates arthritis. J Clin Invest *124*, 3945-3959.

Blank, U., Launay, P., Benhamou, M., and Monteiro, R.C. (2009). Inhibitory ITAMs as novel regulators of immunity. Immunol Rev *232*, 59-71.

Dambuza, I.M., and Brown, G.D. (2015). C-type lectins in immunity: recent developments. Curr Opin Immunol *32*, 21-27.

Deng, Z., Ma, S., Zhou, H., Zang, A., Fang, Y., Li, T., Shi, H., Liu, M., Du, M., Taylor, P.R.*, et al.* (2015). Tyrosine phosphatase SHP-2 mediates C-type lectin receptor-induced activation of the kinase Syk and anti-fungal TH17 responses. Nat Immunol *16*, 642-652.

Duthie, M.S., Raman, V.S., Piazza, F.M., and Reed, S.G. (2012). The development and clinical evaluation of second-generation leishmaniasis vaccines. Vaccine *30*, 134-141.

Furukawa, A., Kamishikiryo, J., Mori, D., Toyonaga, K., Okabe, Y., Toji, A., Kanda, R., Miyake, Y., Ose, T., Yamasaki, S., and Maenaka, K. (2013). Structural analysis for glycolipid recognition by the C-type lectins Mincle and MCL. Proc Natl Acad Sci USA *110*, 17438-17443.

Hamerman, J.A., Ni, M., Killebrew, J.R., Chu, C.L., and Lowell, C.A. (2009). The expanding roles of ITAM adapters FcRgamma and DAP12 in myeloid cells. Immunol Rev *232*, 42-58.

Iborra, S., Izquierdo, H.M., Martinez-Lopez, M., Blanco-Menendez, N., Reis e Sousa, C., and Sancho, D. (2012). The DC receptor DNGR-1 mediates cross-priming of CTLs during vaccinia virus infection in mice. J Clin Invest *122*, 1628-1643.

Iborra, S., and Sancho, D. (2015). Signalling versatility following self and non-self sensing by myeloid C-type lectin receptors. Immunobiology *220*, 175-184.

Ishikawa, E., Ishikawa, T., Morita, Y.S., Toyonaga, K., Yamada, H., Takeuchi, O., Kinoshita, T., Akira, S., Yoshikai, Y., and Yamasaki, S. (2009). Direct recognition of the mycobacterial glycolipid, trehalose dimycolate, by C-type lectin Mincle. J Exp Med *206*, 2879-2888.

Ishikawa, T., Itoh, F., Yoshida, S., Saijo, S., Matsuzawa, T., Gonoi, T., Saito, T., Okawa, Y., Shibata, N., Miyamoto, T., and Yamasaki, S. (2013). Identification of distinct ligands for the C-type lectin receptors Mincle and Dectin-2 in the pathogenic fungus Malassezia. Cell Host Microbe *13*, 477-488.

Karttunen, J., Sanderson, S., and Shastri, N. (1992). Detection of rare antigen-presenting cells by the lacZ T-cell activation assay suggests an expression cloning strategy for T-cell antigens. Proc Natl Acad Sci U S A *89*, 6020-6024.

Kerscher, B., Willment, J.A., and Brown, G.D. (2013). The Dectin-2 family of C-type lectin-like receptors: an update. Int Immunol *25*, 271-277.

Kerscher, B., Wilson, G.J., Reid, D.M., Mori, D., Taylor, J.A., Besra, G.S., Yamasaki, S., Willment, J.A., and Brown, G.D. (2016). Mycobacterial receptor, Clec4d (CLECSF8, MCL), is coregulated with Mincle and upregulated on mouse myeloid cells following microbial challenge. Eur J Immunol *46*, 381-389.

Lefèvre, L., Lugo-Villarino, G., Meunier, E., Valentin, A., Olagnier, D., Authier, H., Duval, C., Dardenne, C., Bernad, J., Lemesre, J.L.*, et al.* (2013). The C-type lectin receptors dectin-1, MR, and SIGNR3 contribute both positively and negatively to the macrophage response to Leishmania infantum. Immunity *38*, 1038-1049.

Leon, B., Lopez-Bravo, M., and Ardavin, C. (2007). Monocyte-derived dendritic cells formed at the infection site control the induction of protective T helper 1 responses against Leishmania. Immunity *26*, 519-531.

Lobato-Pascual, A., Saether, P.C., Fossum, S., Dissen, E., and Daws, M.R. (2013). Mincle, the receptor for mycobacterial cord factor, forms a functional receptor complex with MCL and FcepsilonRI-gamma. Eur J Immunol *43*, 3167-3174.

Martinez-Lopez, M., Iborra, S., Conde-Garrosa, R., and Sancho, D. (2015). Batf3-dependent CD103+ dendritic cells are major producers of IL-12 that drive local Th1 immunity against Leishmania major infection in mice. Eur J Immunol *45*, 119-129.

Matsumoto, M., Tanaka, T., Kaisho, T., Sanjo, H., Copeland, N.G., Gilbert, D.J., Jenkins, N.A., and Akira (1999). A novel LPS-inducible C-type lectin is a transcriptional target of NF-IL6 in macrophages. J Immunol *163*, 5039-5048.

Miyake, Y., Masatsugu, O.H., and Yamasaki, S. (2015). C-Type Lectin Receptor MCL Facilitates Mincle Expression and Signaling through Complex Formation. J Immunol *194*, 5366-5374.

Miyake, Y., Toyonaga, K., Mori, D., Kakuta, S., Hoshino, Y., Oyamada, A., Yamada, H., Ono, K., Suyama, M., Iwakura, Y.*, et al.* (2013). C-type lectin MCL is an FcRgamma-coupled receptor that mediates the adjuvanticity of mycobacterial cord factor. Immunity *38*, 1050-1062.

Ng, L.G., Hsu, A., Mandell, M.A., Roediger, B., Hoeller, C., Mrass, P., Iparraguirre, A., Cavanagh, L.L., Triccas, J.A., Beverley, S.M.*, et al.* (2008). Migratory dermal dendritic cells act as rapid sensors of protozoan parasites. PLoS Pathog *4*, e1000222.

Pagán, A.J., Peters, N.C., Debrabant, A., Ribeiro-Gomes, F., Pepper, M., Karp, C.L., Jenkins, M.K., and Sacks, D.L. (2013). Tracking antigen -specific CD4 +T cells throughout the course of chronic Leishmania majorinfection in resistant mice. Eur J Immunol *43*, 427-438.

Pasquier, B., Launay, P., Kanamaru, Y., Moura, I.C., Pfirsch, S., Ruffié, C., Hénin, D., Benhamou, M., Pretolani, M., Blank, U., and Monteiro, R.C. (2005). Identification of FcalphaRI as an inhibitory receptor that controls inflammation: dual role of FcRgamma ITAM. Immunity *22*, 31-42.

Peters, N., and Sacks, D. (2006). Immune privilege in sites of chronic infection: Leishmania and regulatory T cells. Immunol Rev *213*, 159-179.

Ribeiro-Gomes, F.L., Peters, N.C., Debrabant, A., and Sacks, D.L. (2012). Efficient capture of infected neutrophils by dendritic cells in the skin inhibits the early anti-leishmania response. PLoS Pathog *8*, e1002536.

Sancho, D., Joffre, O.P., Keller, A.M., Rogers, N.C., Martínez, D., Hernanz-Falcón, P., Rosewell, I., and Reis e Sousa, C. (2009). Identification of a dendritic cell receptor that couples sensing of necrosis to immunity. Nature *458*, 899-903.

Sancho, D., and Reis e Sousa, C. (2012). Signaling by Myeloid C-Type Lectin Receptors in Immunity and Homeostasis. Annu Rev Immunol *30*, 491-529.
Sancho, D., and Reis e Sousa, C. (2013). Sensing of cell death by myeloid C-type lectin receptors. Curr Opin Immunol *25*, 46-52.

Schoenen, H., Bodendorfer, B., Hitchens, K., Manzanero, S., Werninghaus, K., Nimmerjahn, F., Agger, E.M., Stenger, S., Andersen, P., Ruland, J.*, et al.* (2010). Cutting Edge: Mincle Is Essential for Recognition and Adjuvanticity of the Mycobacterial Cord Factor and its Synthetic Analog Trehalose-Dibehenate. J Immunol *184*, 2756-2760.

Seifert, L., Werba, G., Tiwari, S., Giao Ly, N.N., Alothman, S., Alqunaibit, D., Avanzi, A., Barilla, R., Daley, D., Greco, S.H.*, et al.* (2016). The necrosome promotes pancreatic oncogenesis via CXCL1 and Mincle-induced immune suppression. Nature *532*, 245-249.

Shenderov, K., Barber, D.L., Mayer-Barber, K.D., Gurcha, S.S., Jankovic, D., Feng, C.G., Oland, S., Hieny, S., Caspar, P., Yamasaki, S.*, et al.* (2013). Cord Factor and Peptidoglycan Recapitulate the Th17-Promoting Adjuvant Activity of Mycobacteria through Mincle/CARD9 Signaling and the Inflammasome. J Immunol *190*, 5722-5730.

Sousa, M.d.G., Reid, D.M., Schweighoffer, E., Tybulewicz, V., Ruland, J., Langhorne, J., Yamasaki, S., Taylor, P.R., Almeida, S.R., and Brown, G.D. (2011). Restoration of pattern recognition receptor costimulation to treat chromoblastomycosis, a chronic fungal infection of the skin. Cell Host Microbe *9*, 436-443.

Srivastav, S., Kar, S., Chande, A.G., Mukhopadhyaya, R., and Das, P.K. (2012). Leishmania donovani exploits host deubiquitinating enzyme A20, a negative regulator of TLR signaling, to subvert host immune response. J. Immunol. *189*, 924-934.

Takai, T., Li, M., Sylvestre, D., Clynes, R., and Ravetch, J.V. (1994). FcR gamma chain deletion results in pleiotrophic effector cell defects. Cell *76*, 519-529.

Walker, P.S., Scharton-Kersten, T., Krieg, A.M., Love-Homan, L., Rowton, E.D., Udey, M.C., and Vogel, J.C. (1999). Immunostimulatory oligodeoxynucleotides promote protective immunity and provide systemic therapy for leishmaniasis via IL-12- and IFN-gamma-dependent mechanisms. Proc Natl Acad Sci USA *96*, 6970-6975.

Wells, C.A., Salvage-Jones, J.A., Li, X., Hitchens, K., Butcher, S., Murray, R.Z., Beckhouse, A.G., Lo, Y.-L.-S., Manzanero, S., Cobbold, C.*, et al.* (2008). The macrophage-inducible C-type lectin, mincle, is an essential component of the innate immune response to Candida albicans. J Immunol *180*, 7404-7413.

Wevers, B.A., Kaptein, T.M., Zijlstra-Willems, E.M., Theelen, B., Boekhout, T., Geijtenbeek, T.B., and Gringhuis, S.I. (2014). Fungal engagement of the C-type lectin mincle suppresses dectin-1-induced antifungal immunity. Cell Host Microbe *15*, 494-505.

Woelbing, F., Kostka, S.L., Moelle, K., Belkaid, Y., Sunderkoetter, C., Verbeek, S., Waisman, A., Nigg, A.P., Knop, J., Udey, M.C., and von Stebut, E. (2006). Uptake of Leishmania major by dendritic cells is mediated by Fcgamma receptors and facilitates acquisition of protective immunity. J Exp Med *203*, 177-188.

Wuthrich, M., Wang, H., Li, M., Lerksuthirat, T., Hardison, S.E., Brown, G.D., and Klein, B. (2015). F. pedrosoi-induced Th17-cell differentiation in mice is fostered by Dectin-2 and suppressed by Mincle recognition. Eur J Immunol.

Yamasaki, S., Ishikawa, E., Sakuma, M., Hara, H., Ogata, K., and Saito, T. (2008). Mincle is an ITAM-coupled activating receptor that senses damaged cells. Nat Immunol *9*, 1179-1188.

Yamasaki, S., Matsumoto, M., Takeuchi, O., Matsuzawa, T., Ishikawa, E., Sakuma, M., Tateno, H., Uno, J., Hirabayashi, J., Mikami, Y.*, et al.* (2009). C-type lectin Mincle is an activating receptor for pathogenic fungus, Malassezia. Proc Natl Acad Sci USA *106*, 1897-1902.

Yazdanbakhsh, M., and Sacks, D.L. (2010). Why does immunity to parasites take so long to develop? Nat Rev Immunol *10*, 80-81.

Figure legends

Figure 1. *Leishmania* releases a soluble ligand for Mincle. (A) Dot blots for Mincle-Fc (top) or control-Fc (bottom) with membranes spotted with fresh or boiled soluble *Leishmania* extracts (SLA) (left) or supernatants (SN) (right) from the indicated dilutions of stationary cultured parasites. Culture medium (none) or TDM were used as controls. (B) ELISA with Mincle-Fc of different doses of SLA or supernatants (fresh or boiled) from *L. major* promastigotes and controls (none or TDB). (C) NFAT reporter activity in response to 10^6, 10^5 or 10^4 of plated lysed-*Leishmania* or TDB in B3Z cells expressing human Mincle-CD3ζ chimera, WT mouse Mincle receptor co-expressing Syk and FcRγ, or the parental cells. (D) NFAT reporter activity in B3Z cells expressing WT mouse Mincle receptor, FcRγ, and Syk and exposed to plated TDB in the presence of the indicated dilutions of fresh or boiled SLA. (E) Staining with anti-Mincle (left) and fluorochrome-labeled SLA on control and Mincle-expressing. (A, E) Data are from one representative experiment of four (A) or three (E) performed. (B, C, D) Bars show arithmetic mean + SEM corresponding to three independent experiments. * $p < 0.05$; ** $p < 0.01$; *** $p < 0.001$ (one way ANOVA with Bonferroni post-hoc test).

Figure 2. The *Leishmania* ligand for Mincle is proteinaceous and present at all parasite stages. (A) Mincle-Fc and Dectin-1-Fc staining with Hoechst 33258 counterstaining in live *L. major* promastigotes or paraformaldehyde (PF)-fixed parasites permeabilized with NP-40. (B) Mean fluorescence intensity in fixed and permeabilized *L. major* promastigotes stained with Dectin-1-Fc (Control-Fc) or Mincle-Fc preincubated with titrated dilutions of anti-Mincle (clone 2F2), isotype control antibody (mouse IgM), or TDM (10 µg/ml starting dose, 3 fold dilution). Bars show arithmetic mean + SEM corresponding to three independent experiments. * $p < 0.05$; ** $p < 0.01$;

*** $p < 0.001$ (one-way ANOVA with Bonferroni post-hoc test). (C) Fixed and permeabilized *L. major* promastigotes were subjected to the indicated treatments (colors) or untreated (black) and stained with Mincle-Fc chimera. Gray histograms show Dectin-1-Fc staining. (D, E) Confocal images of Mincle-Fc and Dectin-1-Fc staining in fixed and permeabilized *Leishmania* promastigotes (D) and bone-marrow-derived macrophages preincubated with promastigotes (E). Nuclei are counterstained with DAPI. Scale bar: 5 μm. (A, C-E) Plots and images are from single representative experiments of three performed.

Figure 3. Mincle deficiency increases resistance to cutaneous leishmaniasis. Flow cytometry analysis of Mincle expression in the indicated cell subsets isolated from ears of naive or *L. major*-infected WT or *Clec4e*$^{-/-}$ mice 1d p.i. MoDC, monocyte-derived DC. Histograms show representative data from three independent experiments (n=9). (C) Time profiles of lesion diameter in the ear pinnae of WT and *Clec4e*$^{-/-}$ mice infected i.d. with 1000 *L. major* parasites. Data arithmetic means ± SEM from a representative experiment (n=16) of three performed. (D, E) Parasite load in the ear (D) and dLNs (E) of WT and *Clec4e*$^{-/-}$ mice at the indicated times after i.d. infection in the ear with 5 x 10^4 *L. major* parasites. Squares show individual data and horizontal bars show arithmetic means from a representative experiment of three performed. (F) Left: In vivo imaging of mouse ears at the indicated times after i.d. inoculation with 5 x 10^4 mCherry$^+$ *L. major* metacyclic promastigotes. Right: Progression of fluorescence signal (pixel/second/cm^2/sr) expressed as arithmetic mean ± SEM (n=6). (C-F) * $p < 0.05$; ** $p < 0.01$; *** $p < 0.001$ (Student's t test at each time point).

Figure 4. Increased adaptive response and enhanced CD4$^+$ T cell priming during *L. major* infection in Mincle-deficient mice. (A-B) WT and *Clec4e*$^{-/-}$ mice were infected

i.d. in the ear with 5 x 10^4 *L. major* parasites. (A) IFN-γ production in $CD4^+$ T cells in response to polyclonal restimulation of ear infiltrates at the indicated times. Left: representative plots 3 weeks p.i. Right: individual data and arithmetic means. (B) IFN-γ in supernatants from dLN cells extracted at the indicated times and restimulated with SLA. Data are arithmetic means + SEM (n=6) of one representative experiment of three performed. (C-D) WT and *Clec4e*$^{-/-}$ mice were transferred with $CD45.1^+$ OTII OVA-specific T cells labeled with Cell Violet and infected i.d. in the ear with 5 x 10^4 particles of either *L. major*, *L. major* expressing OVA (*L. major*-OVA), or recombinant vaccinia virus expressing OVA (VACV-OVA). (C) Left: Representative histograms showing Cell Violet dilution in OTII cells in dLNs, 4 days p.i. Right: Representative plots of Cell Violet dilution and IFN-γ production following *ex vivo* restimulation with OVA peptide. (D) Quantification of IFN-γ^+ OT-II absolute numbers in the dLNs. (E) Mice were vaccinated in the ear with 1 x 10^5 freeze-thawed (F-T) parasites and transferred with OTII as in (C). Quantification of OTII cells that were IFN-γ^+ in the dLNs upon *ex vivo* restimulation with OVA peptide. (F-G) WT and *Clec4e*$^{-/-}$ mice were vaccinated i.d. in the ear with F-T *L. major* and challenged with live parasites in the same site 4 weeks later. (F**)** IFN-γ production in $CD4^+$ effector T cells in the ear upon restimulation as in (A)**,** assessed 2 weeks p.i. (G) Parasite load in the infected ears was evaluated 4 weeks p.i. (A, D, E, F, G) individual data and arithmetic mean of a representative experiment of three performed. * $p < 0.05$; ** $p < 0.01$; *** $p < 0.001$: (A-E) Student's t test; (F, G) one way ANOVA with Bonferroni post-hoc test.

Figure 5. Enhanced DC activation and migration to dLNs after *L. major* infection in Mincle-deficient mice. (A) IFN-γ in supernatants of T cells from healed *L. major*-infected mice after co-culture for 3 d with $CD11c^+$ cells recovered from the dLNs of

WT and *Clec4e*$^{-/-}$ mice 2 d p.i. Data are arithmetic means + SEM from two independent experiments (n=6). (B) Left panels: Representative histograms of CD40, CD86 and CCR7 staining in MoDCs ($CD11b^+Ly6C^+CD11c^+MHCII^+$ gated cells) from ears of infected mice. Right panels: Mean fluorescence intensity (MFI) of CD40, CD86 and CCR7 expression on MoDCs. (C) Representative dot plots (Upper) and frequencies (Lower) of CD11c- and CD40-positive cells in dLNs from uninfected mice or 24 h after *L. major* infection in the ear. (D) Ears of mice inoculated with PBS in the left ear and *L. major* parasites (10^5) in the right ear were FITC painted (see Methods) and dLNs were harvested 24h later. Left : Representative plots of dLN cells gated for CD11c and stained with anti-CD40 and FITC. Right: frequencies of $FITC^+$ $CD11c^+$ dLN cells. (B-D) Individual data and arithmetic means corresponding to a representative experiment of two (B) or three (C, D) performed. (A-D) * $p < 0.05$; ** $p < 0.01$; *** $p < 0.001$ (Student's t test).

Figure 6. Mincle and SHP1 inhibit DC activation by freeze-thawed *L. major*. (A) Histogram overlays for CD40 and CCR7 in $CD11c^+$ GM-DCs from WT and *Clec4e*$^{-/-}$ mice left untreated (gray histograms) or treated with freeze-thawed (F-T) *L. major*. Data are representative of three independent experiments (n=6). (B-D) Fold induction of MFI for CD40 and CCR7 upon F-T *L. major* treatment of (B) GM-DCs obtained from WT, *Clec4e*$^{-/-}$, and CD11cΔ*Syk* mice; (C) WT and *Clec4d*$^{-/-}$ GM-DCs transduced with empty vector, MCL, or MCL^{WAA}; and (D) GM-DCs from WT and CD11cΔ*SHP1* mice. (E) IL-12p40 and TNFα in culture supernatants 20h after exposure of WT, *Clec4e*$^{-/-}$, and CD11cΔ*SHP1* GM-DCs to different doses of F-T *L. major*. Data are arithmetic means + SEM of three independent experiments. (F-G) WT, *Clec4e*$^{-/-}$, and CD11cΔ*SHP1* mice inoculated with 5 x 10^4 *L. major* parasites i.d. in the ear were sacrificed 3 weeks after infection. (F) Parasite load in the infected ear and dLNs. (G) Top: intracellular IFN-γ in

$CD4^+$ T cells after polyclonal restimulation of ear infiltrates. Bottom: IFN-γ in supernatants after SLA restimulation of 2 x 10^6 dLN cells. Data are arithmetic means+ SEM of three independent experiments. (B, D, F, G) Individual data and arithmetic mean corresponding to one representative experiment of three performed; (C) Pooled data from three independent experiments (n=6). (B-G) * $p < 0.05$; ** $p < 0.01$; *** $p < 0.001$ (B, E-G) one way ANOVA with Bonferroni post-hoc test; (C, D) Student's t test.

Figure 7. *L. major* promotes a Mincle/FcRγ/SHP1 axis that impairs DC activation. (A) Western blot (WB) for P-SHP1 and total SHP1 in WT and *Clec4e*$^{-/-}$ GM-DCs lysed at the indicated times of stimulation with F-T *L. major*. (B) SHP1 immunoprecipitation and WB for SHP1, FcRγ and Mincle in WT and *Fcer1g*$^{-/-}$ GM-DCs lysed at the indicated times of stimulation with F-T *L. major*. (C) Mincle immunoprecipitation in B3Z cells transduced with mouse Mincle (Clec4e), Syk, and either WT FcRγ chain or the Y65F (left) or Y76F mutants (right). WB for Mincle, FcRγ and SHP1. (D) Fold induction of MFI for CD40 and CCR7 upon LPS stimulation (200 ng/ml) of F-T *L. major*-pretreated for 30 min (+) or non-pretreated (-) GM-DCs from WT, *Clec4e*$^{-/-}$ and CD11cΔ*Syk* mice. ** $p < 0.01$; Student's t test comparing F-T *L. major* pretreatment and no pretreatment within each genotype. (E) Syk (upper blots) and SHP1 (lower blots) immunoprecipitation from F-T *L. major*-treated WT and *Fcer1g*$^{-/-}$ GM-DCs and WB for Syk and Mincle (upper) or SHP1 and Mincle (lower). (F) SHP1 immunoprecipitation from F-T *L. major*-treated WT and CD11cΔ*Syk* GM-DCs and WB for SHP1 and Mincle. (A-F) Western Blots are from single representative experiments of at least three performed.

Figure 1

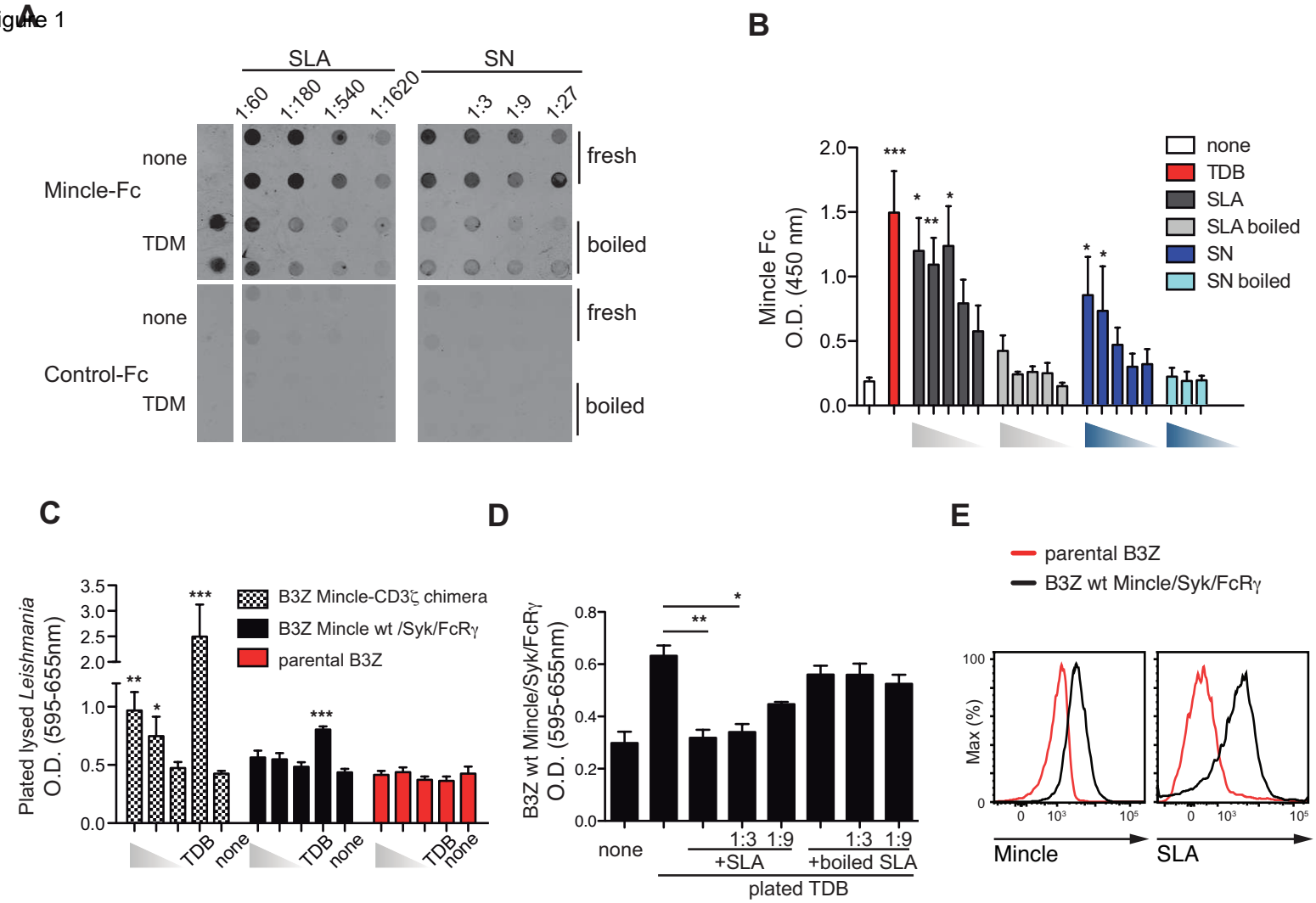

Figure 1

Figure 2

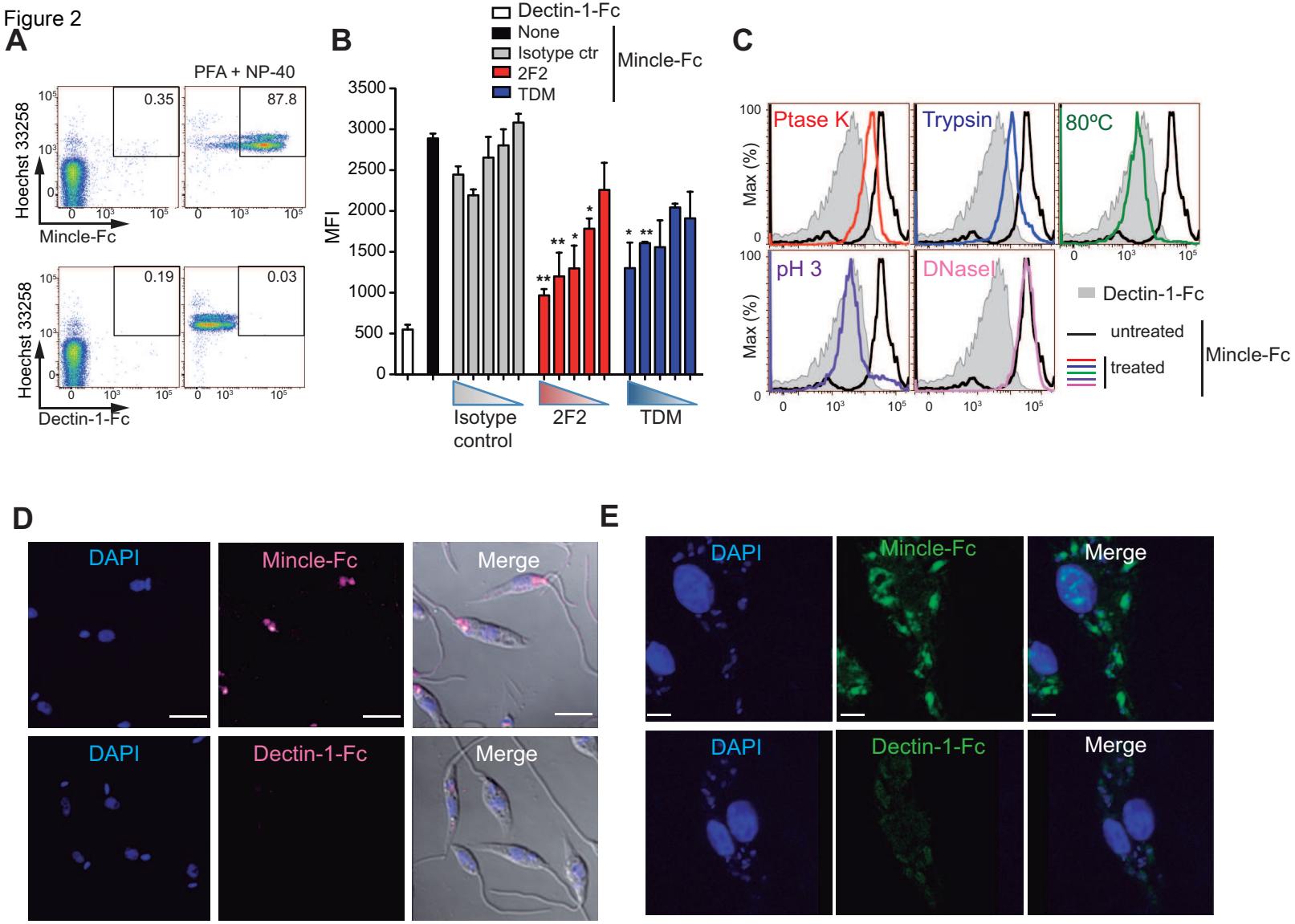
A
PFA + NP-40
0.35
87.8
0.19
0.03
Hoechst 33258
Mincle-Fc
Dectin-1-Fc
B
Dectin-1-Fc
None
Isotype ctr
2F2
TDM
Mincle-Fc
MFI
Isotype control
2F2
TDM
C
Ptase K
Trypsin
80ºC
pH 3
DNaseI
Max (%)
Dectin-1-Fc
untreated
treated
Mincle-Fc
D
DAPI
Mincle-Fc
Merge
DAPI
Dectin-1-Fc
Merge
E
DAPI
Mincle-Fc
Merge
DAPI
Dectin-1-Fc
Merge

Figure 3

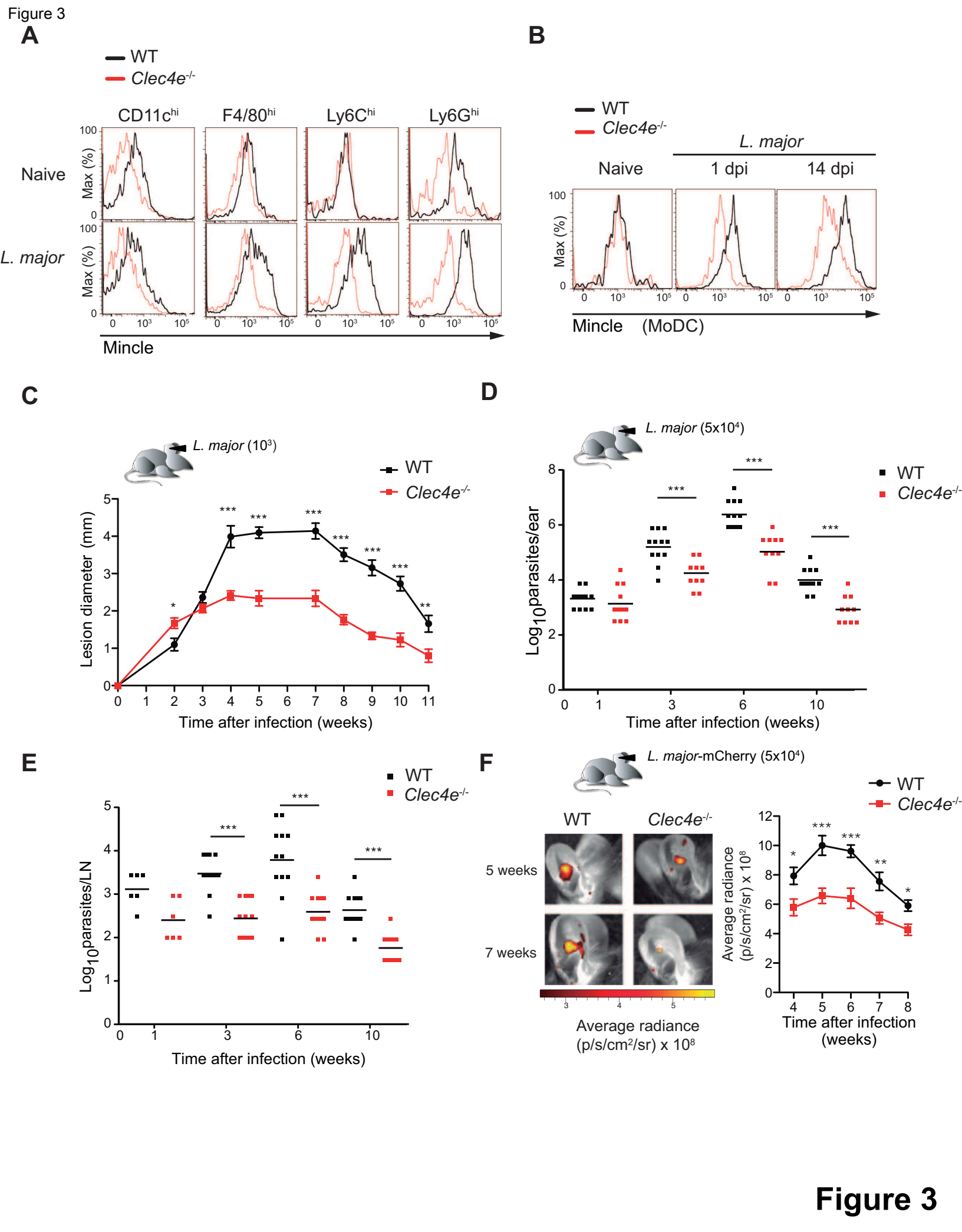

Figure 3

Figure 4

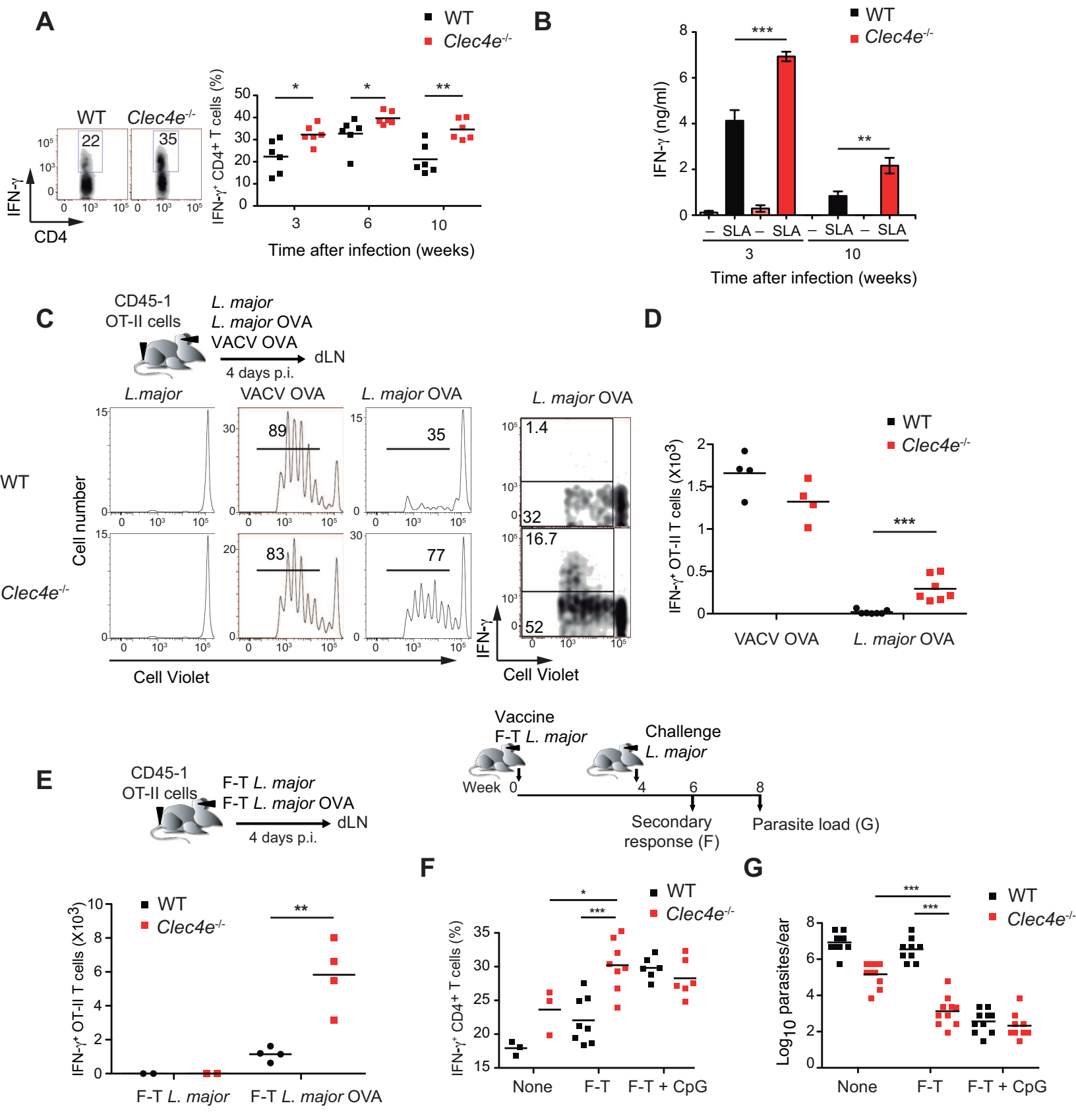

Figure 4

Figure 5

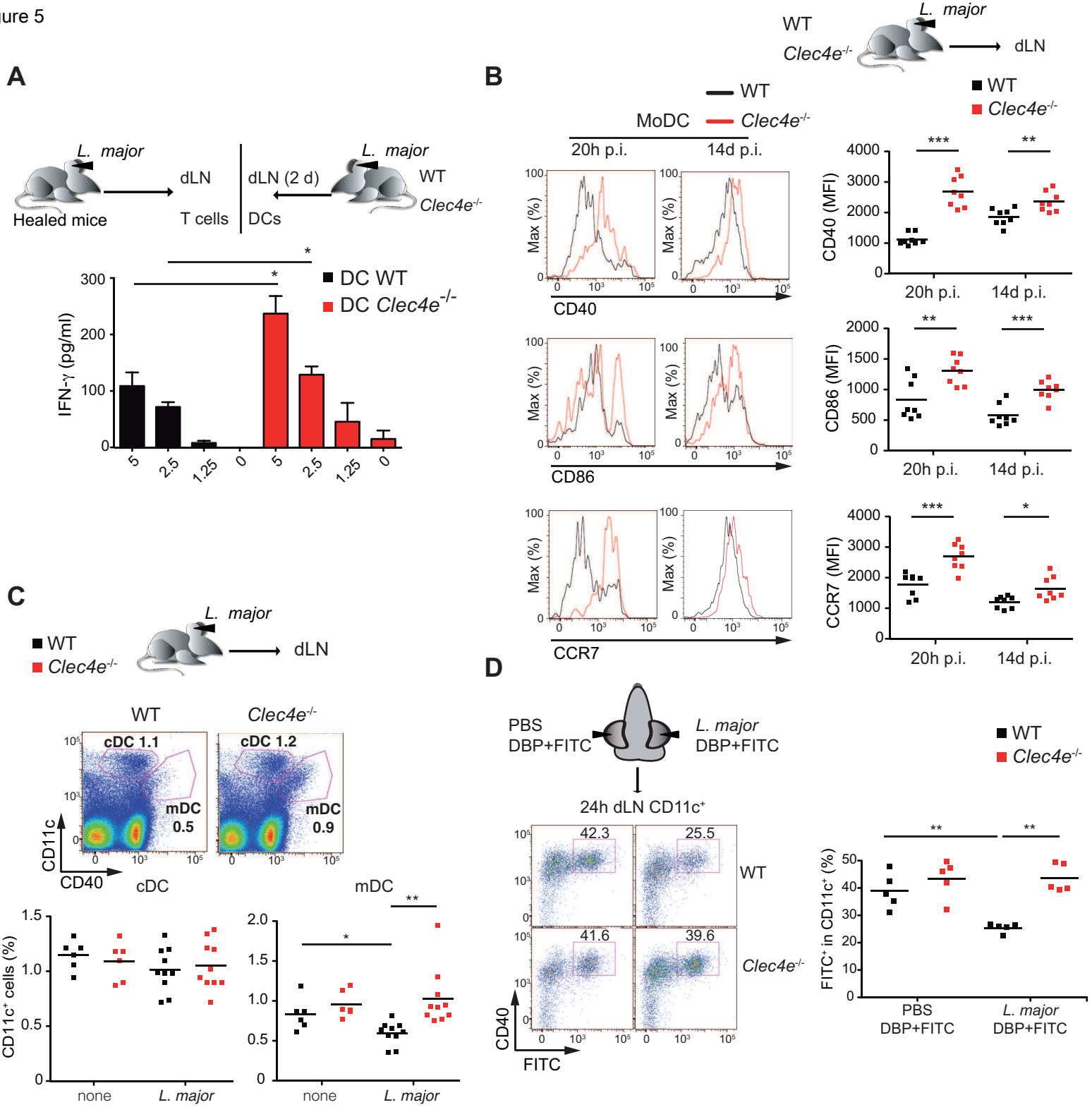

Figure 5

Figure 6

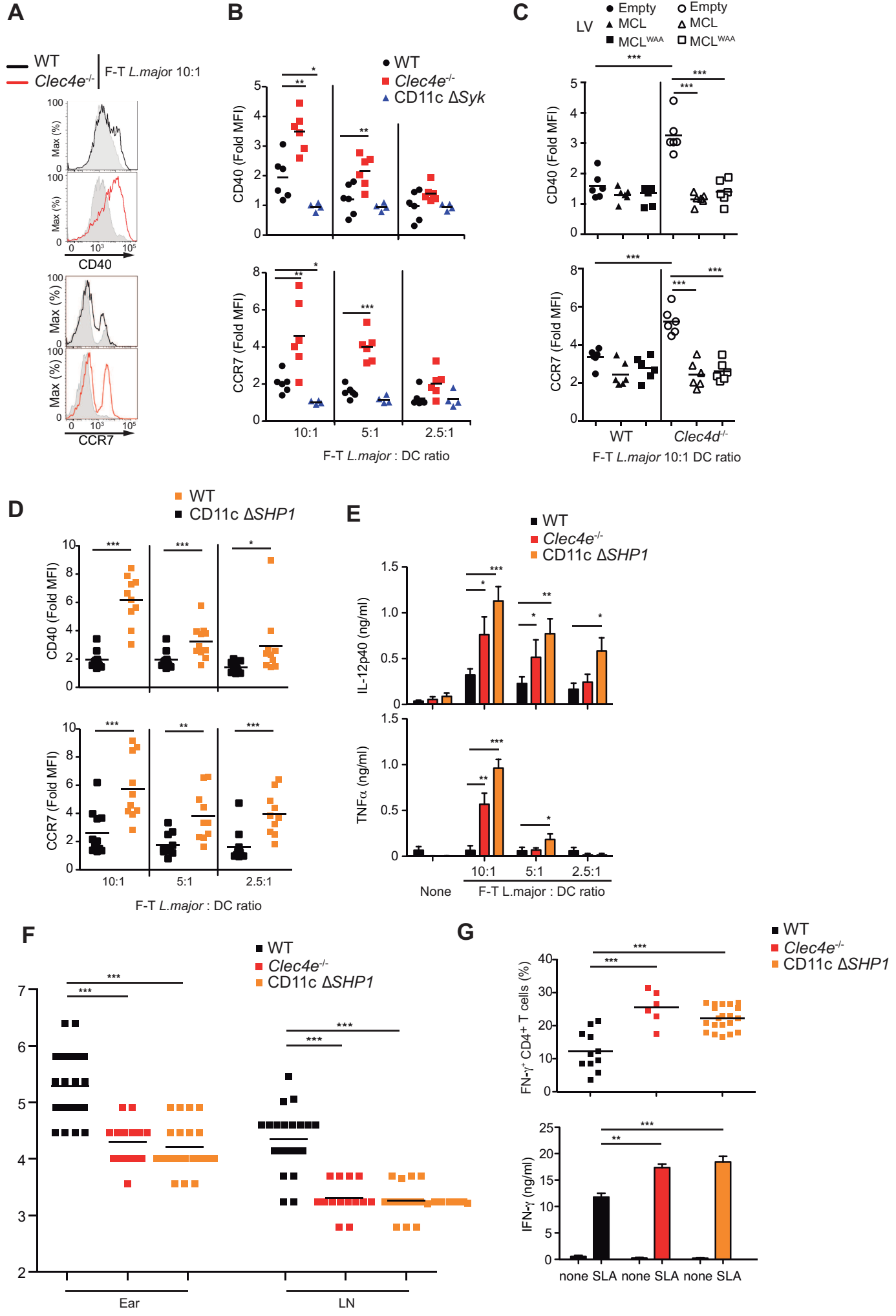

Figure 6

Figure 7

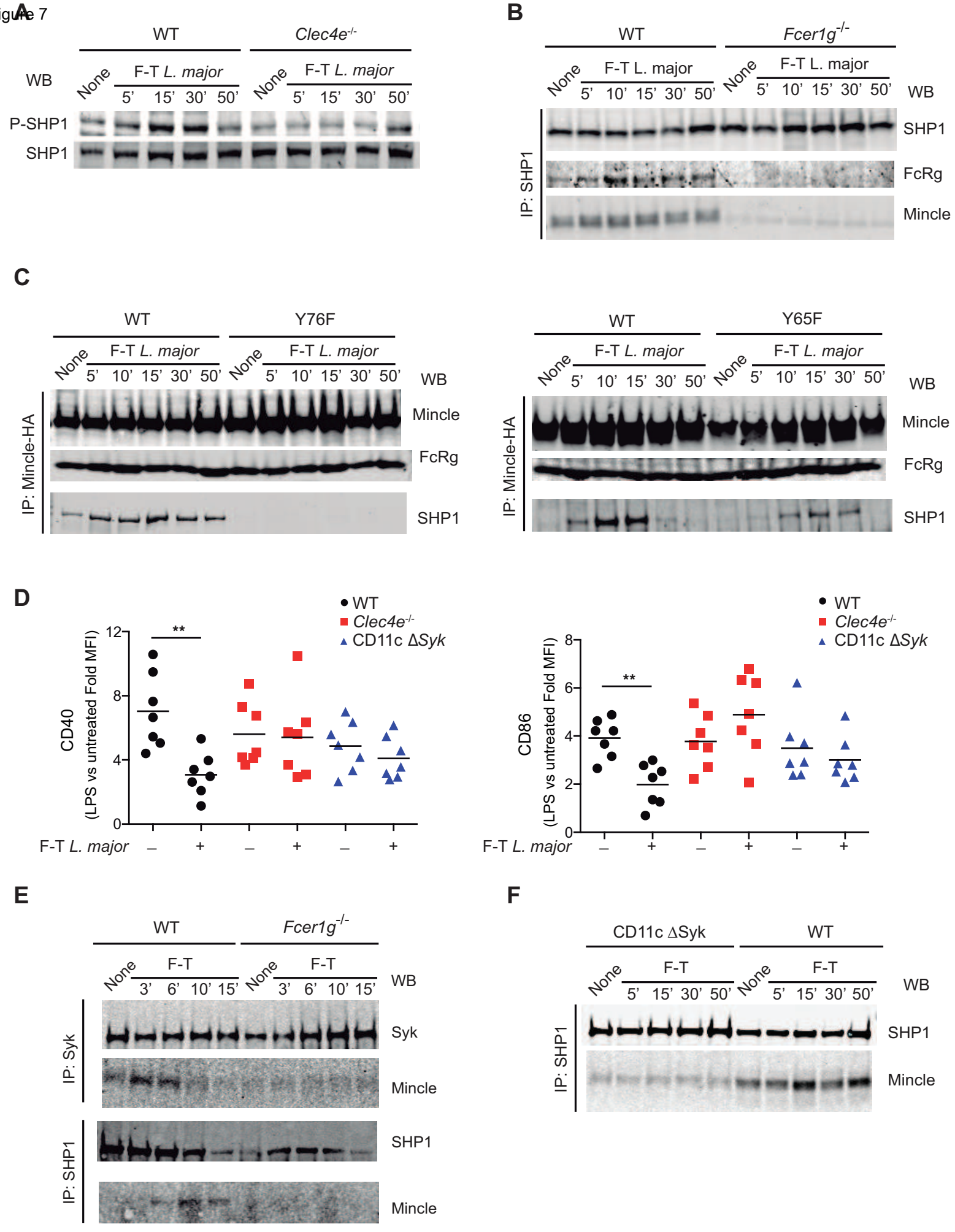

Figure 7

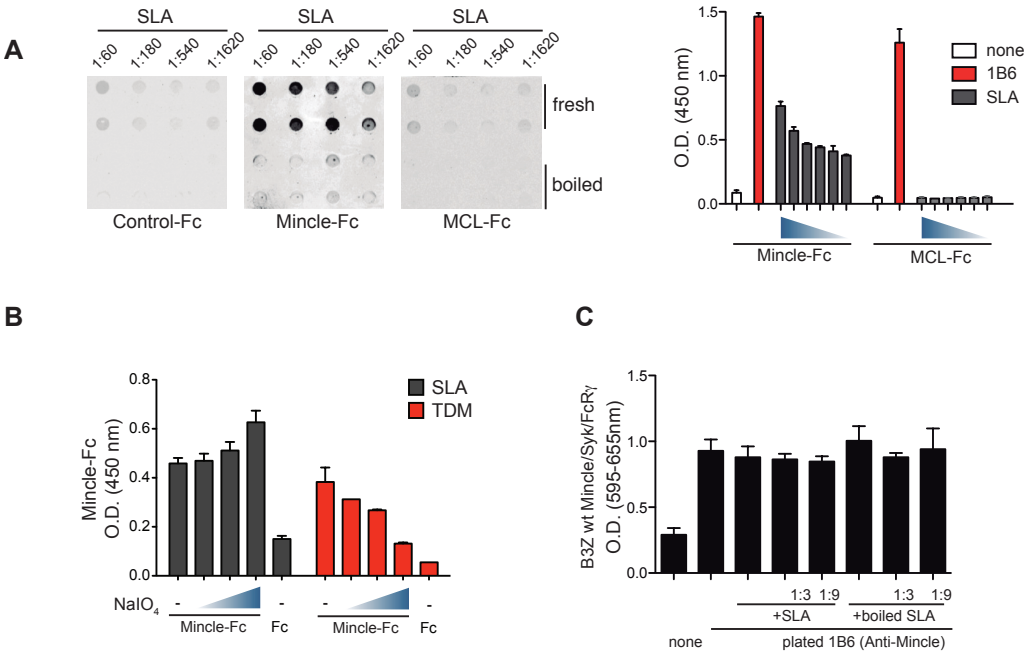

Figure S1 related to Figure 1 (A) *Leishmania* extract was plated and detected by dot blot (left) or ELISA (right) using Mincle-Fc, MCL-Fc, or control-Fc. Plated 1B6 was used as a positive control for ELISA. (B) Plated *Leishmania* extract and TDM were treated with sodium periodate and detected by ELISA using Mincle-Fc or control-Fc. (A-B) Representative experiments are shown of three performed. (C) B3Z reporter cells expressing WT mouse Mincle were exposed to plated 1B6 anti-mouse/human Mincle in the presence or absence of the indicated dilutions of fresh or boiled *Leishmania* extract (SLA). Data are presented as arithmetic mean + SEM corresponding to three independent experiments.

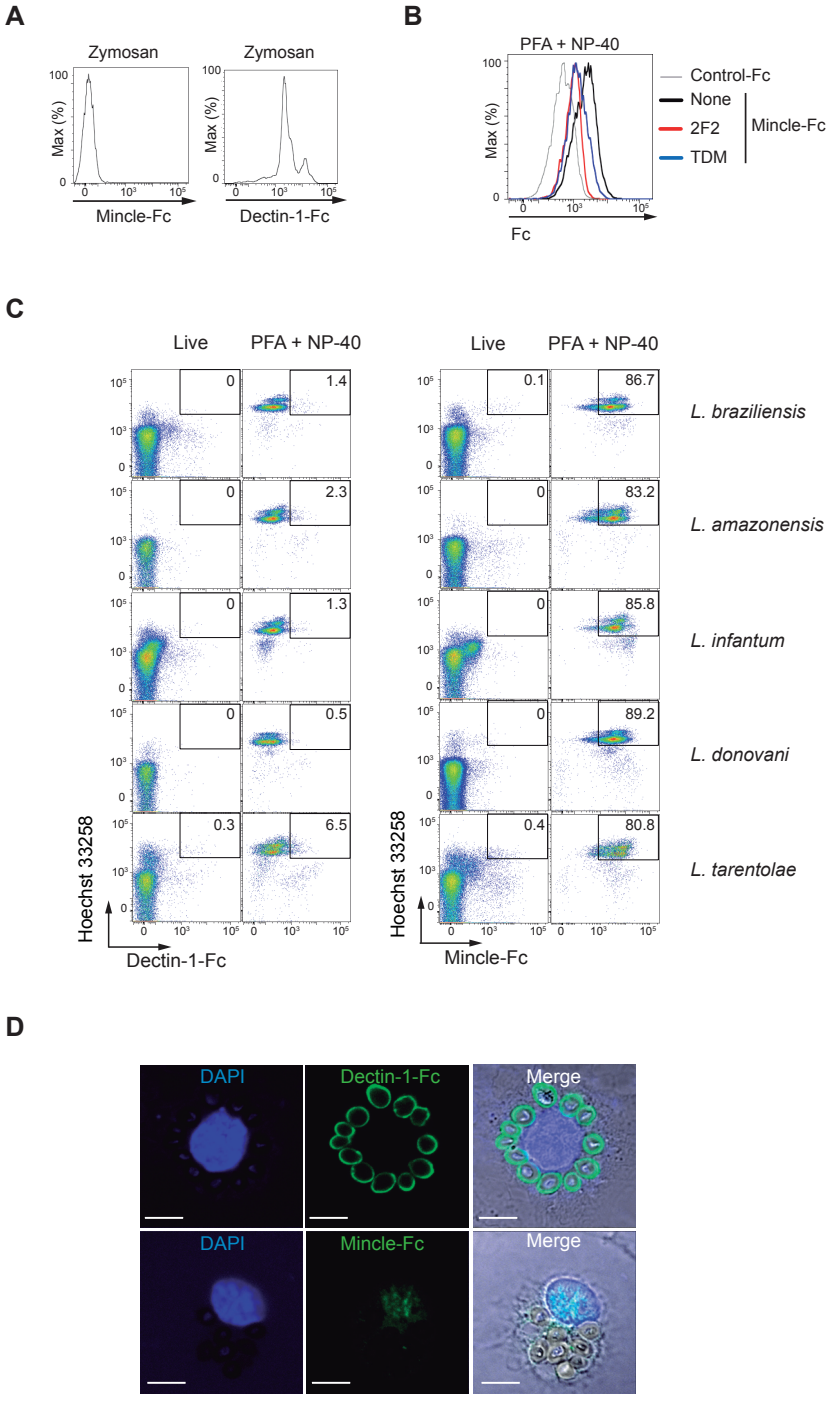

Figure S2, related to Figure 2 (A) Staining of zymosan with Mincle-Fc or Dectin-1-Fc. (B) Staining of freeze-thawed (F/T) *L. major* with control-Fc or Mincle-Fc preincubated or not (none) with 2F2 or TDM. (C) Dectin-1-Fc or Mincle-Fc and Hoechst 33258 staining of live or fixed and permeabilized (PFA + NP-40) promastigotes of different *Leishmania* species. (D) Confocal microscopy images of Dectin-1-Fc and Mincle-Fc staining in fixed and permeabilized zymosan-preincubated bone-marrow-derived macrophages. Nuclei were counterstained with DAPI. Scale bar: 5 µm. (A-D) Single representative experiments are shown of three performed.

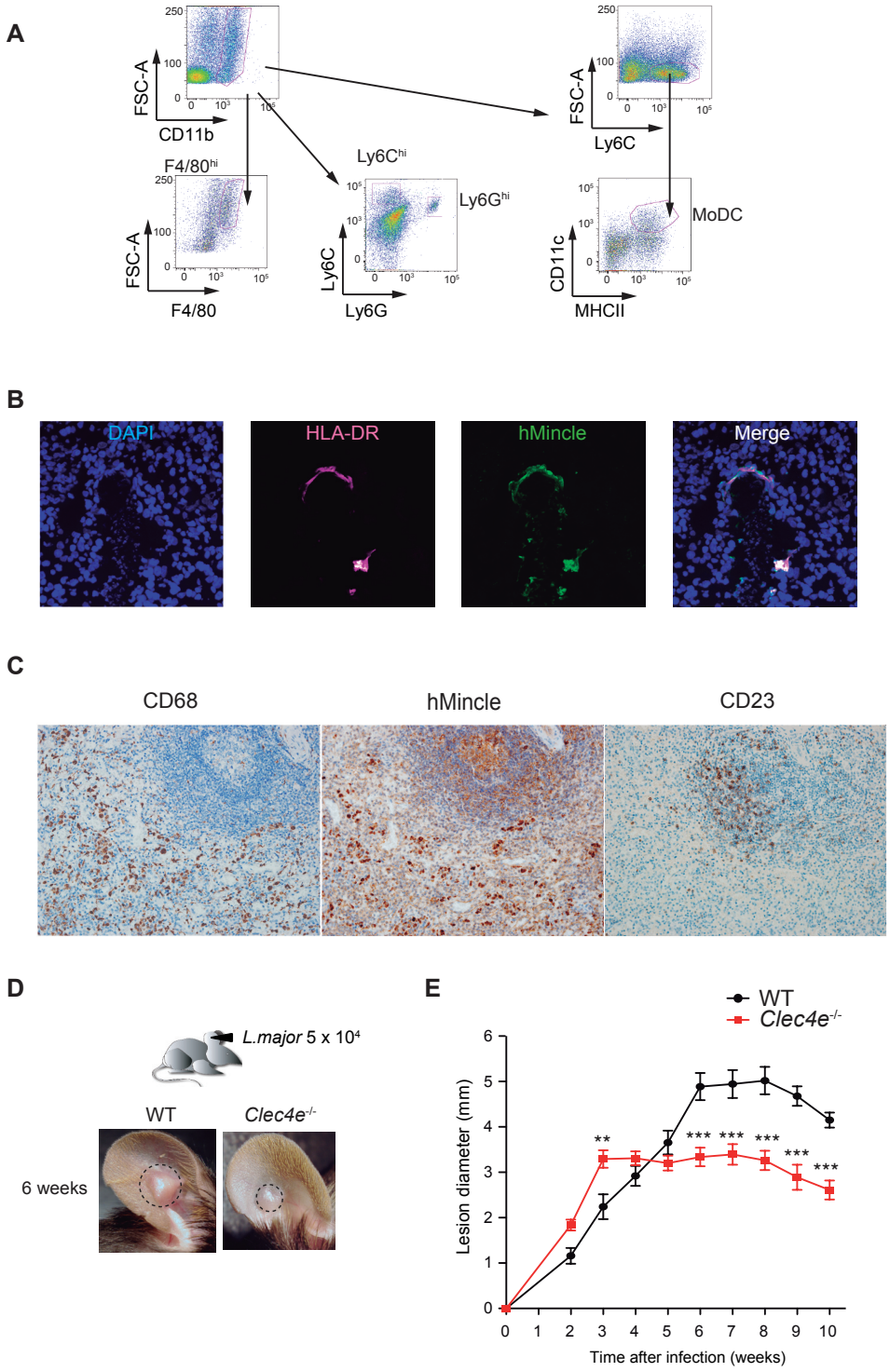

Figure S3 related to Figure 3. (A) Gating strategy used in Figure 3A and B. (B) Immunofluorescence of human skin infected with *L. infantum* and labeled with anti-HLA-DR and anti-human Mincle (1B6). (C) Spleen samples from *L. infantum*-infected individuals immunostained with antibodies to human Mincle (2A8), CD68, and CD23. (B, C) Single representative stainings are shown of three performed. (D, E) Pathology in WT and *Clec4e*$^{-/-}$ mice was tracked for 10 weeks after i.d. infection in the ear pinnae with 5 x 10^4 *L. major* parasites. (D) Representative pictures at 6 weeks p.i. (E) Evolution of lesion size in WT and *Clec4e*$^{-/-}$ mice. Data are arithmetic means ± SEM of 16 samples from a representative experiment of three performed. ** $p < 0.01$; *** $p < 0.001$ (Student's t test).

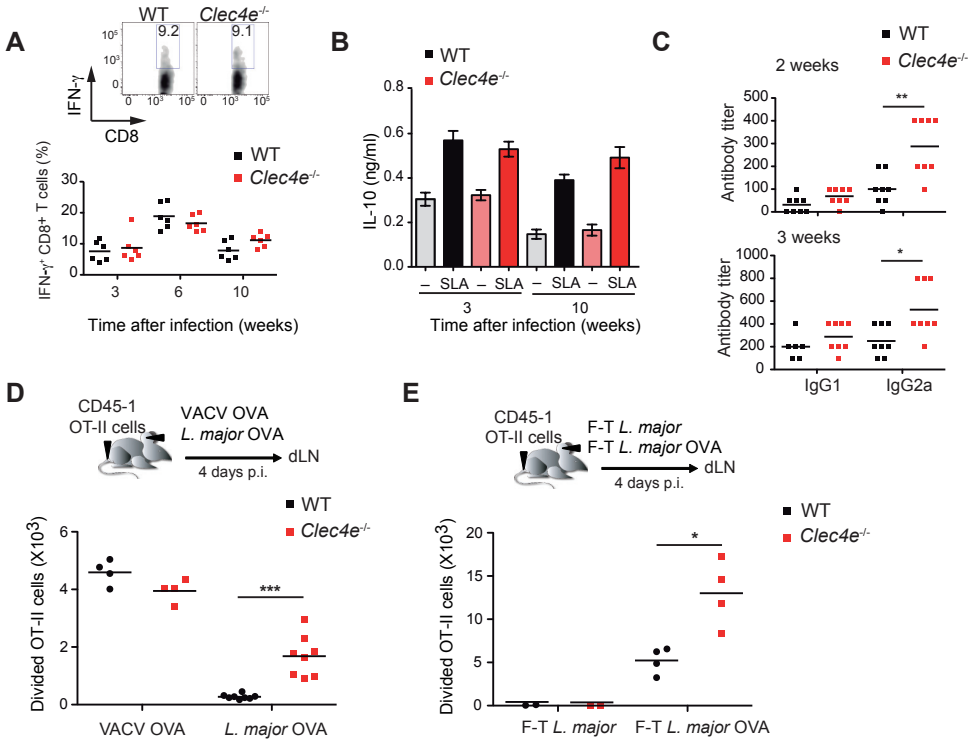

Figure S4 related to Figure 4. (A-C) WT and *Clec4e*$^{-/-}$ mice were infected i.d. in the ear with 5 x 10^4 *L. major* parasites. (A) IFN-γ production by $CD8^+$ T cells after polyclonal restimulation of ear infiltrates at the indicated times. Upper panels: representative plots 3 weeks p.i. Lower panel: Frequency of IFN-γ^+ in $CD8^+$ T cells in the ear. (B) IL-10 in supernatants from dLN cells obtained at the indicated times and restimulated with SLA. Data are arithmetic means ± SEM (n=6) from one representative experiment of three performed. (C) Specific antibody response titer at the indicated times p.i., expressed as the inverse of the positive limiting dilution. (D) WT and *Clec4e*$^{-/-}$ mice were transferred with Cell-Violet-labeled $CD45.1^+$ OTII OVA-specific T cells and infected i.d. in the ear with 5 x 10^4 *L. major* expressing OVA (*L. major*-OVA) or recombinant vaccinia virus expressing OVA (VACV-OVA). Quantification of divided OT-II absolute numbers in the dLN 4 d.p.i. (E) Mice were vaccinated in the ear with 1 x 10^5 F/T parasites and transferred with OTII as in Figure 4E. Dividing OTII cells in the dLN 4 d.p.i. (A, C, D, E) Panels show individual data and arithmetic means of a representative experiment of three performed. * $p < 0.05$; ** $p < 0.01$; *** $p < 0.001$; Student's t test.

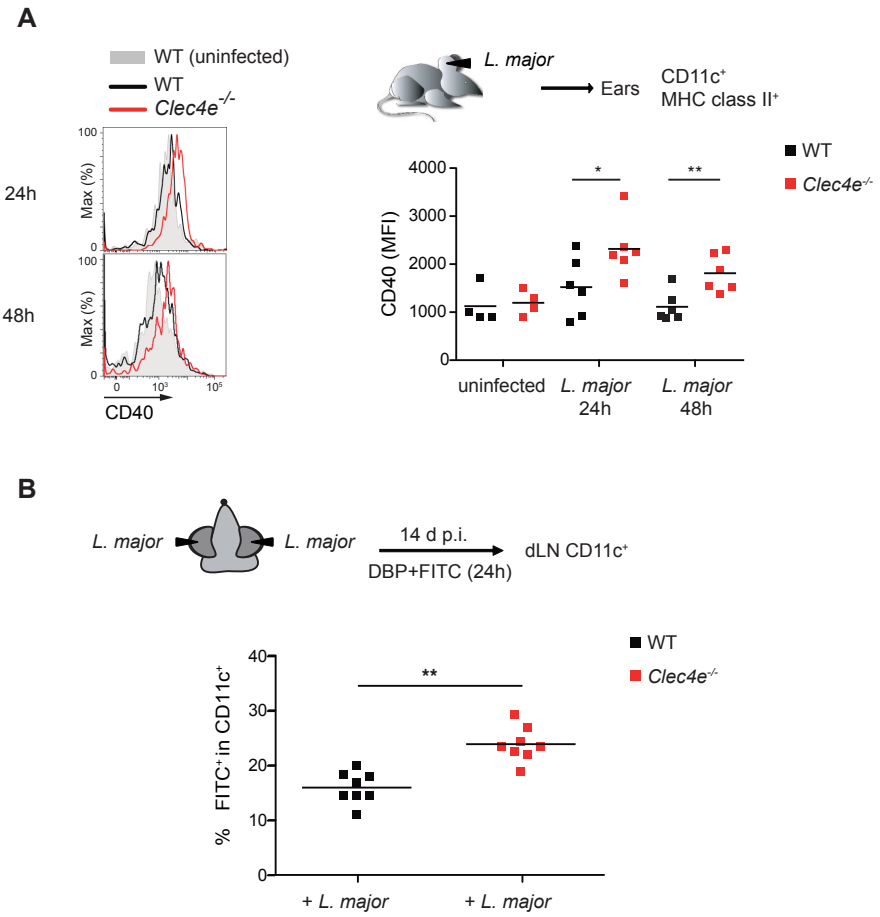

Figure S5 related to Figure 5. (A) Expression of CD40 in ear-infiltrating CD11c$^+$ MHC class II$^+$ DCs at the indicated times after i.d. infection with *L. major* (10^5) in WT and *Clec4e*$^{-/-}$ mice. Left: Representative histograms. Gray, noninfected WT; black, infected WT; red, infected *Clec4e*$^{-/-}$. Right: CD40 MFI. None, noninfected. (B) Mice were inoculated with *L. major* parasites (10^5) in both ears; 14 days later, the ears of mice were painted with FITC prepared in acetone and dibutyl-phthalate (DBP). dLNs were harvested 24h after painting, and FITC$^+$ cells were analyzed in the CD11c$^+$ compartment. (A, B) Panels show individual data and arithmetic means of a representative experiment of three performed; * $p < 0.05$; ** $p < 0.01$; *** $p < 0.001$ (Student's t test).

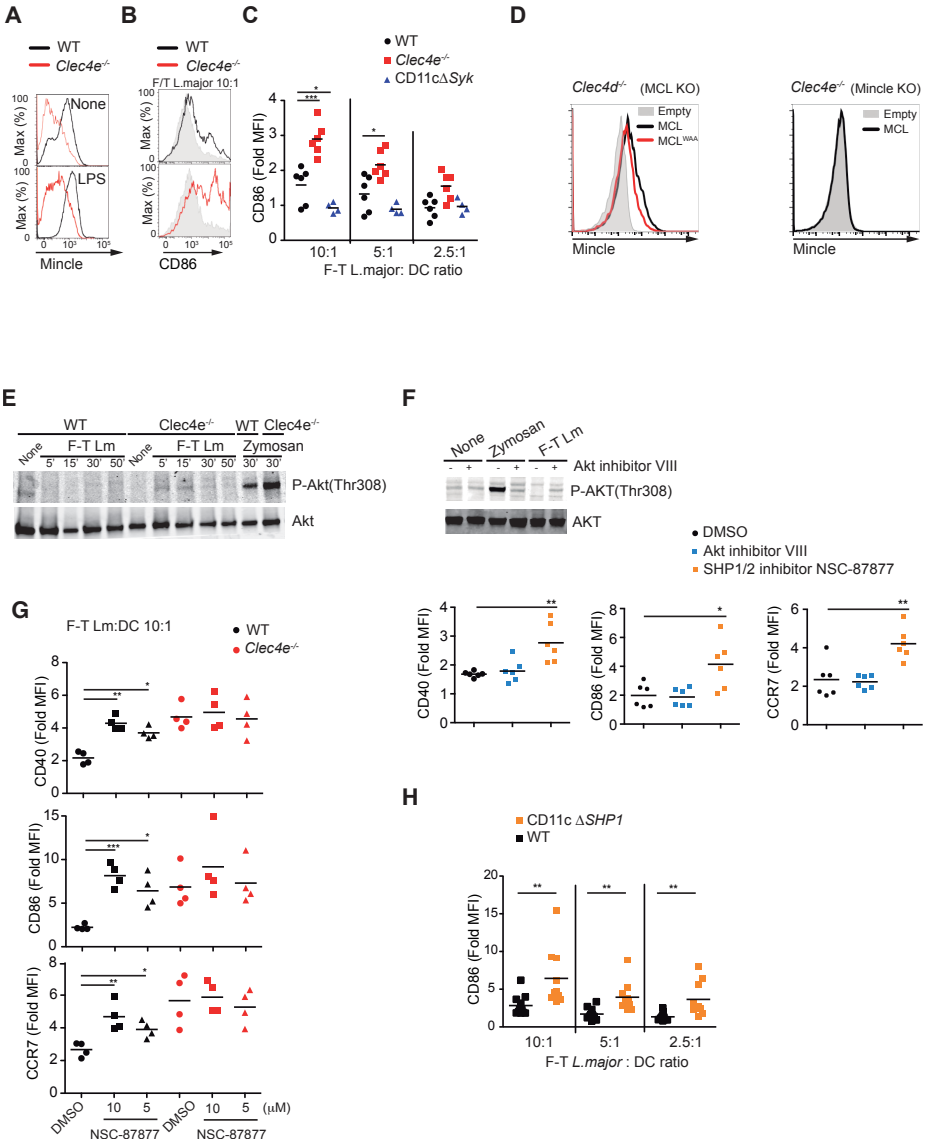

Figure S6 related to Figure 6. (A) Staining of Mincle in untreated and LPS-treated GM-DCs derived from WT and *Clec4e*$^{-/-}$ mice. (B) Representative histogram overlays comparing CD86 induction by freeze-thawed (F-T) *L. major* inWT and *Clec4e*$^{-/-}$ GM-DCs (10:1 *L. major* to DC ratio). Gray histograms show unstimulated cell staining. (C) CD86 expression on GM-DCs from the indicated genotypes exposed to F/T *L. major* at the indicated ratios and expressed as fold induction of MFI compared to resting DCs. (D) Staining with anti-Mincle of MCL-deficient (*Clec4d*$^{-/-}$, left) and Mincle-deficient (*Clec4e*$^{-/-}$, right) GM-DCs transduced with lentiviruses expressing empty vector, MCL or MCL^{WAA}. Representative staining of four independent cultures and transductions.
(E) Western blots for P-Akt (Thr308) and total Akt in GM-DCs from WT and Mincle-deficient (Clec4e-/-) mice treated or not (none) with F/T *L. major* or zymosan for the indicated times. A representative experiment is shown of two performed. (F) Upper panel: WB for P-Akt (Thr308) and total Akt in GM-DCs untreated (none) or treated for 30 min with zymosan or F-T *L. major* (F-T Lm) in the presence (+) or absence (-) of the Akt inhibitor VIII (0.75 μM). Lower panels: Staining of CD40, CD86, and CCR7 in GM-DCs pre-treated with DMSO, Akt inhibitor VIII (0.75 μM) or SHP1/2 inhibitor NSC-87877 (5 μM) and exposed to F-T *L. major* (10:1 ratio to DCs) for 30 min. Results are expressed as fold MFI induction compared *L. major*-treated with untreated. (G) Staining of CD40, CD86, and CCR7 on GM-DCs from WT and *Clec4e*$^{-/-}$ mice untreated or treated with F-T *L. major* (10:1 ratio to DCs) in the presence or absence of the SHP1/2 inhibitor NSC-87877 at the indicated dose. (H) Fold-induction of CD86 in GM-DCs in response to F-T *L. major* compared to resting DCs in WT and CD11cΔ*SHP1* mice. (C, F-H) Panels show individual data and arithmetic mean corresponding to one representative experiment of three performed. * $p < 0.05$; ** $p < 0.01$; *** $p < 0.001$ (Student's t test).

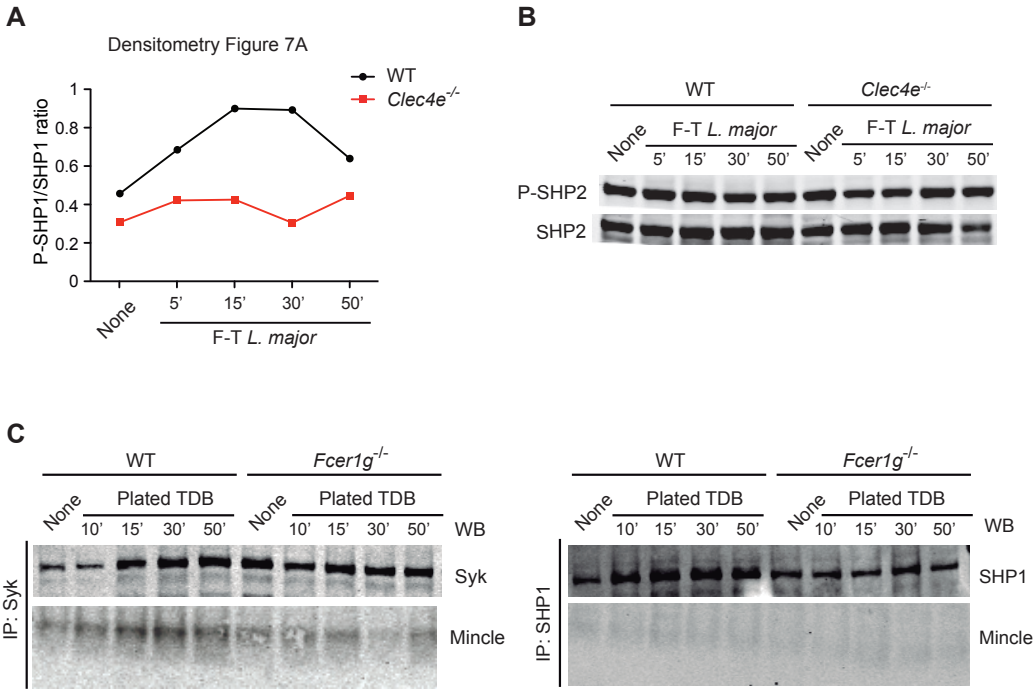

Figure S7 related to Figure 7. (A) Densitometry corresponding to Figure 7A. (B) Western blot for phospho-SHP2 and total SHP2 in CD11c^{+} GM-DCS, as in Figure 7A. A representative experiment is shown of three performed. (C) Immunoprecipitation with anti-Syk (left) or anti-SHP1 (right) in GM-DCs generated from WT or FcRγ chain-deficient mice (*Fcer1g*$^{-/-}$) and treated or not (None) with plated TDB. WB for Syk and Mincle (left) and SHP1 and Mincle (right). A representative experiment is shown of three performed.

Supplemental Experimental Procedures

Leishmania parasite species

In vivo experiments were carried out using different *L. major* lines*: L. major* Friedlin strain FV1 (MHOM/IL/80/ Friedlin) was generously provided by Dr. D. Sacks (NIH) (Iborra et al., 2011). *L. major* FV1 (MHOM/IL/80/ Friedlin) parasites expressing ovalbumin (*Leishmania*-OVA) were kindly provided by Prof. Deborah Smith and Prof. Paul Kaye (University of York) (Prickett et al., 2006). Recombinant *L. major* LV39c5 (RHO/SU/59/P) parasites expressing the red-fluorescent protein mCherry (mCherry$^+$ *L. major*) were described previously (Calvo-Álvarez et al., 2012). *L. amazonensis* (IFLA/BR/67/pH.8), *L. braziliensis* (MHOM/BR/75/M2904), *L. donovani* (MHOM/IN/83/Dd8), and *L. tropica* (MHOM/SU/74/K27) were generously provided by Dr. J. Moreno (IS Carlos III, Spain). *L. infantum* (MCAN/ES/96/BCN150) was kindly provided by Dr. L.C. Gómez-Nieto (UNEX, Spain).

Cell culture and purification

GMCSF bone marrow derived cells (GM-DCs) were obtained from bone marrow cell suspensions after culture on non-treated 150-mm Petri dishes in the presence of 20 ng.ml-1 recombinant GMCSF (Peprotech, London, UK) as described (del Fresno et al., 2013). After 6-7 days, most cells had a typical DC morphology and phenotype (MHC class II$^+$, CD11c$^+$). GM-DCs were collected on day 8 and purified by positive selection with anti-CD11c-microbeads (Miltenyi Biotec). Bone-marrow-derived macrophages (BMDM) were obtained from bone marrow cell suspensions after culture on non-treated 60-mm Petri dishes in complete RPMI medium supplemented with 20% FCS, 2 mM L-glutamine, 100 U.ml-1 penicillin, 100 µg.ml-1 streptomycin, 50 µM 2-mercaptoethanol, and 30% supernatant of the M-CSF-producing cell line L929. On day 7, preparations of BMDM, characterized as CD11b$^+$ F4/80$^+$ cells, were >95% pure.

Single-cell suspensions of lymph nodes and ears were prepared by liberase/DNAse digestion. When further purification was required of CD4$^+$ T cells from lymph nodes, cell suspensions were negatively selected using a cocktail of biotin-conjugated antibodies (anti-CD11c, CD11b, B220, MHC-II, CD4, NK1.1) followed by separation with Streptavidin-microbeads (Miltenyi Biotec). T cells were restimulated to induce cytokine production by incubation for 6h over plated anti-CD3 (2C11,10 µg/ml) in the presence of soluble anti-CD28 (37.51, 5 µg/ml), and brefeldin A (Sigma, 5 µg/ml) added for the last 4h of culture. DCs from LNs and ears were purified with anti-CD11c-microbeads (Miltenyi Biotec). Cells were then stained with FITC-anti-CD4, PE-anti-CD8α, fixed with 4% PFA, and incubated with APC-anti-IFN-γ during permeabilization with 0.1% saponin. An average of 10^4 of each T cell subset was analyzed in each sample. Background activation obtained with non-pulsed cells (0–0.3%) was subtracted in the statistics. For the detection of the release of IFN-γ and IL-10 specific for *Leishmania* antigens, 3×10^6 cells from dLNs were seeded in 48-well plates at 37ºC for 72 h in the presence or absence of SLA (12 µg ml^{-1}). Cytokine release was measured in culture supernatants by ELISA.

Stimulation of GM-DCs

CD11c$^+$ GM-DCs (2x10^6/ml) were stimulated by co-culture with serial dilutions of freeze-thawed (F/T) *L. major*. Activation was assessed as the upregulation of CD40, CD86, and CCR7 and cytokine release measured by ELISA in CD11c$^+$ GM-DCs from WT mice or mice deficient in Mincle, Syk, SHP1, or FcRγ chain or in the presence of SHP1/2 phosphatase inhibitor (5 or 10 µM, NSC-87877, Calbiochem).

Transduction of GM-DCs with lentiviruses

MCL and its mutant genes were introduced into the CSII- CMV-MCS-IRES-Bsd expression vector. Human embryonic kidney (HEK)293T cells were transfected with the expression vector together with packaging vectors (pCMV-VSV-G-RSV-Rev and pCAG-HIVgp). Culture supernatant was collected at 48–72 h after transfection. Virus was concentrated by ultracentrifugation at 50,000 × g for 2 h at 20 ℃. For transduction, WT, Mincle-deficient or MCL-deficient BMDCs were incubated with lentivirus at a multiplicity of infection empirically determined for each lentivirus that yield to successful transduction tested by blasticidin S resistance, together with 20 µl of DOTAP liposomal transfection reagent (Sigma-Aldrich). After 16 h, the medium was replaced with fresh culture medium. Lentivirus-infected cells were selected by culture with10 µg/ml blasticidin S for 3 d.

Processing of ear tissue and dLNs

At the indicated times after *L. major* infection, ears were harvested from naive or infected mice. The ventral and dorsal sheets of the infected ears were separated and placed in RPMI containing 50 μg/ml Liberase CI enzyme blend (Roche). After 90 min at 37°C, the tissues were cut into small pieces and homogenized. Retromaxillary (auricular) dLNs were removed and mechanically dissociated using tweezers and a syringe plunger. Tissue homogenates were filtered through a 70 μm cell strainer (Falcon Products).

Antibodies and flow cytometry

Samples for flow cytometry were stained in ice-cold PBS supplemented with 2mM EDTA, 1% FCS, 0.2% sodium azide, and the appropriate antibody cocktails. Anti-mouse antibodies to CD45, CD4, CD8α, CD11b, CD11c, CD103, Gr-1, Ly-6C, CCR7, and I-A^b (MHC-II) and anti-human IgG (Fc gamma-specific) conjugated to biotin, FITC, PE, PerCP-Cy5.5, V450, or APC were obtained from eBioscience. APC-Cy7 CD45 was from Tonbo Biosciences. PE-conjugated-anti-mouse Ly-6G was from BD Biosciences. APC-anti-IFN-γ was from Miltenyi Biotec. Purified anti-FcγRIII/II (2.4G2) was used to block non-specific antibody binding. Non cell-permeant Hoechst 33258 (0.1 μM) was used as a counterstain to detect necrotic cells. Mouse Mincle receptor was stained with 1B6 (Medical& Biological Labs.) or rat IgG2b 6G5 (Invivogen) antibodies. For generation of the recombinant human Mincle-Fc chimera, the cDNA encoding human Mincle extracellular domain (amino acid residues 46-219 Swiss-Prot Accession number Q9ULY5) was optimized for mammalian expression and synthesized by Life Technologies. Cysteine residue 52 was replaced by serine to reduce the level of disulphide-linked aggregation seen with the wild type sequence. The cDNA fragment was cloned into the mammalian expression destination vector pDEST12.2 (Invitrogen). The expression vector had been modified to contain regions encoding an N-terminal polyhistidine (His10) and human Fc tag. Mincle-Fc protein was directed for secretion into the medium by the inclusion of a CD33 signal sequence. Human Mincle-Fc was expressed in suspension-adapted CHO cells using polyethylenamine (Polysciences) as the transfection reagent. Recombinant Mincle fusion protein was purified from culture supernatant using Protein A (HiTrap Protein A HP column; GE Healthcare) affinity chromatography followed by size exclusion chromatography (Superdex 75 column; GE Healthcare). Mouse Dectin-1-Fc was generated by cloning the EcoRI-NotI fragment of the PCR product into the EcoRI-NotI sites of the pSecTag.Fc^{mut} vector, which couples to human IgG1 Fc. Primers used were mDectin-1 CTLD Eco Fw 5' TTTCCCGAATTCTCTTGCCTTCCTAATTGGAT 3' and mDectin-1 CTLD Not Rv 5' TTTCCCGCGGCCGCAGTTCCTTCTCACAGATAC 3'. Human IgG1Fc control was from Abcam. To characterize the nature of the *Leishmania* ligand for Mincle, SLA and TDB were plated on ELISA plates, treated with different concentrations of NaIO4 (Sigma) and degradation agents (Proteinase K, 50 μg/ml; trypsin, 0.05%; DNase I, 0.1 mg/ml), and tested with Mincle-Fc or human IgG1Fc. Human Mincle-Fc chimera was blocked with anti-human Mincle 2F2 clone; isotype matched antibody (clone MID 15B4, rat IgM) was used as a control (Sigma). Events were acquired using a FACSCanto flow cytometer and FACSDiva software (Becton Dickinson), and data were analyzed with FlowJo software (Tree Star). Representative plots are shown in the Figures. The percentage of positive cells was calculated and is indicated within dot plots. Each experiment contained a minimum of three biological replicates, and a minimum of three independent experiments was performed. Percentage and mean fluorescence intensity (MFI) data from sets of experiments are graphed as the mean ± SEM. SLA was conjugated to APC using Lightning-Link® APC technology (Innova Biosciences), and adhesion to cellular Mincle on B3z cells was analyzed by flow cytometry.

Immunofluorescence, confocal microscopy, histology, in vivo imaging and ELISA

For immunofluorescence, promastigotes or *L. major*-infected macrophages were adhered to coverslips coated with poly-L lysine (50μg/ml, Sigma) for 30m at 37ºC. Coverslips were washed in PBS, and cells were then fixed in 2% paraformaldehyde in PBS for 10 minutes at room temperature, washed with PBS, and permeabilized with 0.1% Triton X-100 (TX-100) in PBS solution for 10 minutes. Preparations were then incubated with blocking solution (2% skimmed milk, 0.1% TX-100 in PBS) for 60 minutes at room temperature and stained with Fc ectodomains and counterstained with DAPI to reveal nuclei and kinetoplasts. Finally, samples were covered with ProLong Gold Antifade Reagent liquid mountant (Life Techologies) and visualized under a *Zeiss LSM 700* confocal microscope. Human samples of *Leishmania*-infected spleen were collected from the BioB-HVS biobank.

The IVIS Spectrum in vivo imaging system (Perkin Elmer) was used to determine the evolution of parasitemia in real time. Mice were inoculated i.d. in the ear with mCherry+*L. major* (5×10^4), and fluorescence emission was tracked as described (Calvo-Álvarez et al., 2012). mCherry$^+$ *L. major*-infected animals were lightly anesthetized with isoflurane placed in the camera chamber, and the fluorescence signal was acquired for 3 s. Fluorescence determinations were recorded using the Xenogen in vivo imaging system 100. To quantify fluorescence, a region of interest was outlined and analyzed using the Living Image Software Package (version 2.11, Xenogen). Results are expressed as average radiance (photons/s/sr/cm^2).

Antibody pairs for ELISA (IL12p40, IL-6, IL-10 and TNF-α) were from BD, and ELISAs were performed according to the manufacturer's instructions. ELISAs were developed using extravidin®-alkaline phosphatase and pNPP alkaline phosphatase substrate from Sigma.

Western blot analysis and immunoprecipitation

For immunoblotting, $1x10^6$ CD11c$^+$ GM-DCs were seeded in 24 well plates for 4 hours in serum free RPMI and stimulated with dead *Leishmania* at a 10:1 parasite: GM-DC ratio. For immunoprecipitation, $1x10^7$ CD11c$^+$ GM-DCs or $3x10^7$ B3Z cells were stimulated with dead *Leishmania* at a 5:1 ratio. After stimulation, cells were washed and resuspended in Triton X-100 lysis buffe*r* (50 mM Tris-HCl pH 7.5, 1mM EGTA, 1mM EDTA pH 8.0, 50mM NaF, 1mM sodium glycerophosphate, 5mM pyrophosphate, 0.27 M sucrose 0.5 % Triton X-100, 0.1mM PMSF, 0.1% 2-mercaptoethanol, 1mM sodium orthovanadate, and protease inhibitor cocktail (Roche)). After incubation on ice for 15 minutes, nuclei were pelleted by centrifugation for 15 minutes (1,300 × *g*, 4°C). For immunoprecipitation assays, cell extracts were incubated O/N with dynabeads→ bound to 2 μg anti-mouse SHP1 (rabbit polyclonal; Santa Cruz C-19), or 4 μg anti-HA (Miltenyi). After pull-down, beads were washed thrice in ice-cold lysis buffer and eluted by boiling in SDS sample buffer. Cytosolic protein extracts or immunoprecipitated proteins were separated by SDS–PAGE and transferred onto nitrocellulose membrane (Bio-Rad Laboratories). After blocking with 5% bovine serum albumin (fraction V, Sigma), membranes were incubated overnight with antibodies to phospho-SHP1 (Tyr564; #8849), SHP1(#3759), phospho-Syk (Tyr525/526; #2711), Syk (#2712) (Cell Signaling Technology, Danvers, MA); SHP1 (Santa Cruz, sc-7289); Mincle (1B6); or Fcer1g (antibodies online, RB41735). Membranes were imaged with the *LI-COR* Odyssey Infrared Imaging System.

FITC skin sensitization migration assay

Mice were inoculated in the left ear with PBS and in the right ear with *L. major* parasites (5×10^4). Ears were painted 16h or 14 days later with 1% FITC (Sigma-Aldrich) prepared in an inflammatory stimulating solution of acetone and dibutyl-phthalate (1:1, vol:vol) as previously described (Macatonia et al., 1987). Retromaxillary LNs were harvested 24h after painting, and LN cells were analyzed by flow cytometry for CD11c, CD40, and FITC staining.

Supplemental References

Calvo-Álvarez, E., Guerrero, N.A., Álvarez-Velilla, R., Prada, C.F., Requena, J.M., Punzón, C., Llamas, M.Á., Arévalo, F.J., Rivas, L., Fresno, M.*, et al.* (2012). Appraisal of a Leishmania major Strain Stably Expressing mCherry Fluorescent Protein for Both In Vitro and In Vivo Studies of Potential Drugs and Vaccine against Cutaneous Leishmaniasis. PLoS Negl. Trop. Dis. *6*, e1927.

del Fresno, C., Soulat, D., Roth, S., Blazek, K., Udalova, I., Sancho, D., Ruland, J., and Ardavín, C. (2013). Interferon-beta Production via Dectin-1-Syk-IRF5 Signaling in Dendritic Cells Is Crucial for Immunity to C. albicans. Immunity *38*, 1176-1186.

Iborra, S., Soto, M., Stark-Aroeira, L., Castellano, E., Alarcón, B., Alonso, C., Santos, E., and Fernández-Malavé, E. (2011). H-ras and N-ras are dispensable for T-cell development and activation but critical for protective Th1 immunity. Blood *117*, 5102-5111.

Macatonia, S.E., Knight, S.C., Edwards, A.J., Griffiths, S., and Fryer, P. (1987). Localization of antigen on lymph node dendritic cells after exposure to the contact sensitizer fluorescein isothiocyanate. Functional and morphological studies. J Exp Med *166*, 1654-1667.

Prickett, S., Gray, P.M., Colpitts, S.L., Scott, P., Kaye, P.M., and Smith, D.F. (2006). In vivo recognition of ovalbumin expressed by transgenic Leishmania is determined by its subcellular localization. J Immunol *176*, 4826-4833.

Leishmania uses Mincle to target an inhibitory ITAM signaling pathway in dendritic cells that dampens adaptive immunity to infection

Salvador Iborra, María Martínez-López, Francisco J. Cueto, Ruth Conde-Garrosa, Carlos Del Fresno, Helena M. Izquierdo, Clare L. Abram, Daiki Mori, Yolanda Campos-Martín, Rosa María Reguera, Benjamin Kemp, Sho Yamasaki, Matthew J. Robinson, Manuel Soto, Clifford A. Lowell and David Sancho.

Inventory of Supplemental Information

- Main text Figure 1 is supported by Supplemental Figure 1

- Main text Figure 2 is supported by Supplemental Figure 2

- Main text Figure 3 is supported by Supplemental Figure 3

- Main text Figure 4 is supported by Supplemental Figure 4

- Main text Figure 5 is supported by Supplemental Figure 5

- Main text Figure 6 is supported by Supplemental Figure 6

- Main text Figure 7 is supported by Supplemental Figure 7